ISSN : 2800-1729 **Edition :** Vol 3. Num 1 (2024)

Biopolymer Applications Journal

Editor in chief:

Pr. HAMMICHE Dalila

Tasdawit n Bgayet
Université de Béjaïa

UNIVERSITÉ ABDERRAHMANE MIRA - BEJAIA
FACULTÉ DE TECHNOLOGIE

Table of content

Biopolymer Applications Journal **Lilia Benchikh et al. Vol 03. N°1, 2024, pp.01.-07**
e-ISSN: 2800-1729

Cellulose nanocrystals/polyaniline particles's dispersion in polypropylene nanocomposites

Lilia BENCHIKH[1*]; Yazid AITFERHAT[2]; Maya KEBAILI[2], Ilyes ABACHA[2], Melia GUESSOUM[3], Abdelhafid MERZOUKI[3], Yves GROHENS[4]
[1] *Centre de Recherche en Technologies Agroalimentaires. Route de Targa Ouzemmour, Campus Universitaire, Bejaia, 06000. Algeria*
[2]*Centre de recherche en mécanique, Campus Chaab Erssas, Université les frères Mentouri 1, Constantine 25021, Algéria*
[3]*Laboratoire Physico-Chimie des hauts polymères, université Ferhat Abbas, Setif 1, Setif 19000, Algéria*
[4]*Institut de Recherche Dupuy de Lôme, UMR CNRS 6027, Université de Bretagne Sud, Lorient, France*
**Corresponding author email: lilia.benchikh@gmail.com*

Received: 15 November, 2023; Accepted: 16 December, 2023; Published: 22 January, 2024

Abstract

Sustainable development and biomass valorization are a primary means of reducing the non-renewable resources consumption and an opportunity to exploit the agricultural and forestry sectors where biomass as a renewable resource will play an important role. Cellulose is the most abundant bio-renewable material and its unique structure generates nanoparticles known as cellulose nanocrystals (CNC). Cellulose nanomaterials show a great promise for various applications therefore with a relatively low loading level, significant improvements on mechanical properties of nanocomposites could be obtained, but CNCs have a strong tendency to agglomerate and its hydrophilic characteristic leads to interfacial incompatibility with non-polar polymer matrices.

In this work, polyaniline (PANI) is used as a support for Cellulose nanocrystals dispersion on Polypropylene (PP) matrix. Cellulose nanocrystals were obtained according to an experimental protocol at several stages and Polyaniline was deposited on CNC's surface during polyaniline synthesis in CNC's suspension. The obtained CNC/PANI nanoparticles were incorporated into the polypropylene matrix by melting compounding technique. Polypropylene nanocomposites and PANI/CNC particles were characterized with different techniques: FTIR, AFM, electrical conductivity and mechanical properties to study and assess how polyaniline and CNC affect microstructure, morphology and electrical properties of PP. Characterization technique showed that PANI was successfully synthesized on CNC's surface and PANI/CNC material is a semiconductor. The enhanced mechanical properties of PP/PANI-CNC nanocomposites indicates a good dispersion of CNCs particles on PP matrix.

Keywords: *Cellulose nanocrystals, CNC, Polyaniline, Polypropylene, Nanocomposites*

I. Introduction

In the era of sustainable development, it is important to produce high-performance, value-added materials from abundant renewable resources and cellulose from photosynthesis, is the most abundant polymer on earth [1].

Cellulose can be transformed into micro- and nanoscale materials by various chemical, enzymatic and mechanical treatments and depending on their morphology and properties; it consists of cellulose nanocrystals (CNC), nanofibers cellulose (CNF) and bacterial cellulose (BC) [2,3]. Nanocellulose enjoys specific properties such as high aspect ratio, high specific modulus, relatively good surface reactivity and non-toxicity, as well as being readily available, renewable and biodegradable [4]. The variety of dimensions, morphologies, degrees of crystallinity depend on the source of cellulosic material and the conditions under which the preparation is carried out [5]. Nanocellulose is easily accessible nanofiller for the fabrication of novel nanocomposites [6].

Thermoplastics, particularly Polypropylene (PP), are consumed in large quantities. PP is widely used in industry due to its ease of processing, low cost and good overall properties [7,8]. However, PP is largely limited by insufficient strength and poor thermal properties [9].

Therefore, PP is usually loaded by particles and fibers to obtain composites with better properties [10,11].

Polyaniline (PANI) is one of the most common conductive polymers due to its high electrical conductivity, high environmental stability in addition to relatively low cost [12]. Potential uses of polymer/PANI blends are in the areas of electronic components and coatings; and PP/PANI composites can be used as membranes [13,14]. Also, Hybridization of PANI with other materials has been exploited to improve PANI's properties [15].

CNCs have been usually applied as nanoreinforcement in polyolefin, polyester, rubber, polyurethane (WPU), epoxy resins and natural polymers, etc.; and processable nanocomposites of PANI and both CNF and CNC, have successfully been made [16-18]. PANI lignocellulose composites are used as absorbents to remove commonly used dyes, which are non-biodegradable and toxic to humans and environment [17,18].

On the other hand, nonpolar matrices have low interfacial compatibility with polar nanocellulose attributed to the hydrogen bonds on CNCs surface forming agglomerations and requires various methods of modifying fillers or matrices to promote interactions between filler and matrix [19-21]; Among these techniques of modification, casting/evaporation nanocomposites preparation is predominant. In-situ polymerization has also been reported in nanocomposites preparation with polyolefin matrices [22]. This method consists of polymerizing the reactive monomers with the nanoparticles.

In this present work, CNC/PANI nanocomposites were successfully developed by in situ polymerization of aniline in a CNC suspension with the main objective of covering the CNCs surface with PANI in order to reduce the hydrogen bonds between CNCs particles and allow optimal dispersion of PANI-CNC in PP matrix. PP/PANI composites with different PANI-CNC contents (0, 0.5, 1, 2 and 3 wt%) and compatibilized with PP-g-MA were prepared by hot mechanical mixing. The obtained nanocomposite materials were characterized by different structural, mechanical and rheological techniques. CNC-PANI's dispersion state in the PP matrix was also observed by AFM.

II. Material and methods

CNCs were extracted from El Diss (Ampelodesmos mauritanicus). CNCs nanocrystals preparation method and characterization details were reported earlier by Benchikh and al. [23]. The used polypropylene is “HG385MO” produced by "Borouge", with a density of 0.91 g/cm^3 and a melt flow index of 25g/10min (at 230° C and under 2.16 kg). The PP-g-MA used is polybond 3200, a polypropylene grafted with maleic anhydride, commercialized by Cromptan Unioroyal Chemical with a density of 0.91 g/cm^3 and a melt flow index of 11.5g/10min. The reagents used for PANI preparation are : Hydrochloride acid (HCL), aniline, Ammonium persulfate (APS), purchased from CARLO ERBA (Cornaredo, Milan, Italia) and Biochem Chemical Pharma (Montreal, Quebec, Canada).

CNC/PANI nanocomposites were prepared according to the procedure described as follows: An aniline solution was first prepared by dissolving aniline (0.2 mol /l) in concentrated HCl (0.1 M, 37 wt %), and then it was mixed with a 1% CNC suspension to obtain 1L of an homogeneous reaction mixture dispersion (dispersed in an ultrasound bath for 120 min). The obtained aqueous dispersion was put in a vial at low temperature water bath (5°C) under a constant stirring, 0.2 mol/l of APS was added drop by drop during 1h. After polymerization at 5°C for 1h, a dark green suspension was formed. Finally, the suspension was washed several times.

PP/PANI nanocomposite samples were prepared by the hot pressing method. PP/PANI mixtures were obtained by blending PP matrix with PANI-CNC powder in different weight percentages (0, 0.5, 1, 2 and 3% wt) in a Brabender (GmbH & Co.KG, Model 819952, 2010, Germany), at 200 °C for 8 minutes.

II.1. Characterization

A. Fourier transform infrared spectroscopy (FTIR spectroscopy)

To investigate structural modifications after adding PANI-CNC mixture to PP, the obtained PP/PANI-CNC nanocomposites were characterized by FTIR spectroscopy. The samples were analyzed using a Perkin-Elmer (L1600400 Spectrum TWO DTGS) spectrometer, in transmittance mode (4000 cm^{-1}-400 cm^{-1}, 2 cm^{-1}).

B. Atomic force microscopy (AFM)

Atomic force microscopy images were obtained on the different samples using an AFM microscope (contact mode, a tip of 2 Nm^{-1}) and physical characteristics of the observed surfaces from 3-D images were quantified by measuring their roughness on a scanning surface of 10µm×10µm with a dimension of 1552×1254 pixels.

C. Conductivity analysis

For measuring PANI-CNC conductivity, a pellet of (PANI-CNC) is prepared, and using a multimeter, a transverse resistance is measured and converted into volume resistivity. For PP/PANI-CNC nanocomposites, electrical conductivity measurements were carried out using the Van der Pauw technique.

D. Melt flow index

The Melt Flow Index (MFI) is a static method widely used in industry to determine fluidity of a polymer. To carry out this analysis, PP/PANI-CNC samples were subjected to the NF EN ISO 113 standard.

E. Mechanical tests

Tensile properties were evaluated using MTS Landmark® (MTS Systems Corporation (USA)) universal testing machine. Samples were prepared according to ASTM-D 638 and tested at a drawing speed of 5 mm/min. Izod impact strength of nanocomposites was measured by assessing samples of dimensions (62×13×3) mm^3 using a Ceast Resil Impact instrument equipped with a hammer of 1.8 kg delivering an impact energy of 7.5 kJ.

III. Results and discussion

A. Structural characterization

FTIR spectra of PANI-CNC and PP/PANI-CNC nanocomposites are shown in Figure 1.

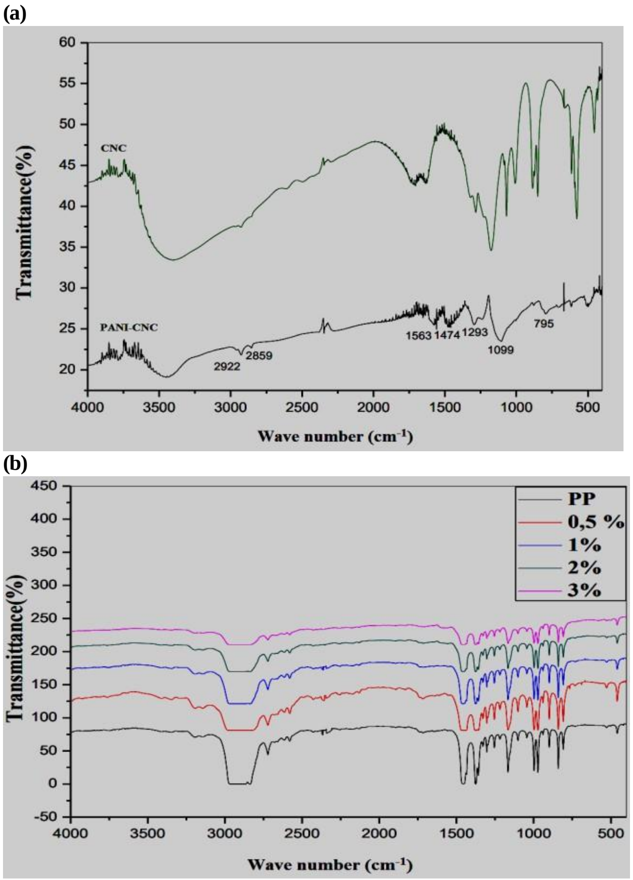

Figure 1. FTIR spectra of : **(a)** CNC-PANI particles, **(b)** PP/CNC-PANI Nanocomposites

The peaks of 1563 and 1474 cm^{-1} came from the elongation vibration of N = Q = N and N-B-N structures, respectively (B and Q represent the fractions benzenoids and quinoids in PANI chains) and confirm that the structures are doped. The peaks at 1293 and 1140 cm^{-1} are assigned to C-N elongation vibration and the in-plane aromatic C-H bending, respectively. The peak corresponding to C-H band out-of-plane bending vibration of the para-disubstituted benzene ring appears at 795 cm^{-1} [24-26]. The peak at 1099 cm^{-1} is linked to NH+ interactions with SO^{3-} [27]. These results conclude that PANI was successfully formed on the surface of cellulose nanocrystals (CNC) during in-situ polymerization.

Figure 1 (b), presents the FTIR spectra recorded on the developed nanocomposites.

From FTIR spectra, it can be deduce that the obtained nanocomposites has the same characteristic peaks of PP. However, in PP/PANI-CNC at 3%, a new band at 3346 cm^{-1} is appeared corresponding to the CNC hydroxyl groups elongation and a band at 1561 cm^{-1} corresponding to quinoid groups elongation of PANI structure [28].

B. Morphological characterization

AFM images of PANI-CNC composites (figure 2) show a rough heterogeneous surface, with dispersed aggregates. The presence of these grains in large quantities is explained by a large quantity of polyaniline, equivalent to two times the quantity of cellulose particles. These results indicate a massive deposition of PANI's particles on CNCs particles or on CNC aggregates.

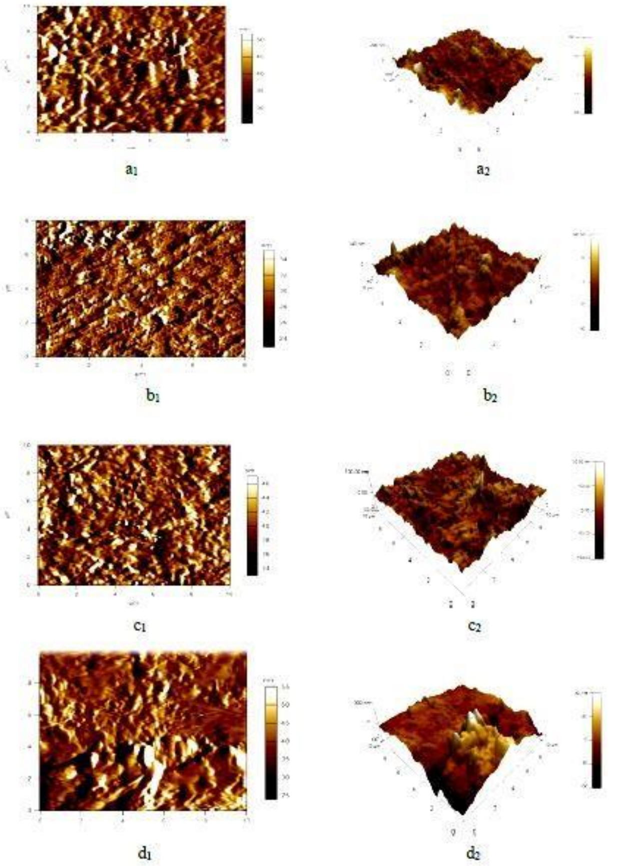

Figure 2. Image AFM of: (a_1, a_2) PANI-CNC, (b_1, b_2) PP, (c_1, c_2) PP/PANI-CNC 1%, (d_1, d_2) PP/PANI-CNC 3%

Surfaces structure evolution (topography) of pure PP and nanocomposites (1 and 3%) are irregular, covered with grains of lateral dimensions and height between 24-34/70-140 nm, 34-36/50-100 nm and 25-55/150 nm to 300 nm for PP, PP/PANI-CNC 1% and PP/PANI-CNC 3%, respectively.

PP/PANI-CNC 1% surface is relatively smooth compared to those of pure PP and PP+3%. In table 1, we have reported the roughness values noted on the materials. PP/PANI-CNC 1% shows a decrease in value of root mean square (RMS) roughness. Reduction of surface roughness can be attributed to a reduction in overall size therefore a good dispersion of filler at low concentration unlike PP at 3% where the roughness increased and can be explained by aggregates formation on the surface.

Table 1. Roughness values of PANI-CNC particles and PP/PANI-CNC nanocomposites

Samples	PANI-CNC	pp	PP+1%	PP+3%
Surface Roughness Measurement (nm)	35	19	16	66

C. Electrochromic Properties

PANI-CNC in powder form, is compressed to obtain a pellet of 13.18 mm in diameter and 4.65 mm in thickness. Transverse resistance is measured and volume resistivity is calculating as follow:

$$\rho = (R*\pi*r2) / e$$

$$R = 0.17\ \Omega,\ r = 1.318\ \text{cm},\ e = 0.465\ \text{cm}$$

$$\rho = 1.99\ \Omega.\text{cm}$$

$$\boldsymbol{\sigma = 1/\rho = 0.50\ \Omega^{-1}\text{cm}^{-1}}$$

The measured conductivity of (PANI-CNC) corresponds to a high range of semiconductors (10^{-4} S/cm < σ semiconductor < 1 S/cm), demonstrating a synthesis of a PANI/CNC composite with electronic properties improved.

According to FTIR characterization, PANI-CNC synthesis by an In-situ process leads to efficient interactions between PANI quinoid ring and CNCs and facilitate the charge transfer processes between the two components [29].

On the other hand, when PANI-CNC particles is used as reinforcement in PP matrix at 0.5% and 1%, it is observed that the conductivity is almost the even. For PP/PANI-CNC 3%wt, where there is a fairly significant conductivity reduction, this has been attributed to polyaniline agglomeration tendency at high rates of loads. Conductive properties of these composites depend on the molecular organization of the conductive aggregates in relation to the polymer matrix and the geometry of the conductive charge, as well as the charge-charge interaction [26]. These results are in agreement with the morphological properties studied by AFM.

Table 2. Conductivity value of PP/PANI-CNC nanocomposites

Samples	Conductivity (10^{+8} S/cm)
PP/PANI-CNC 0.5%	2.11
PP/PANI-CNC 1%	2.01
PP/PANI-CNC 2%	2.32
PP/PANI-CNC 3%	1.63

D. Melt flow index analysis

Fluidity index evolution as a function of load rate is shown in Figure 3.

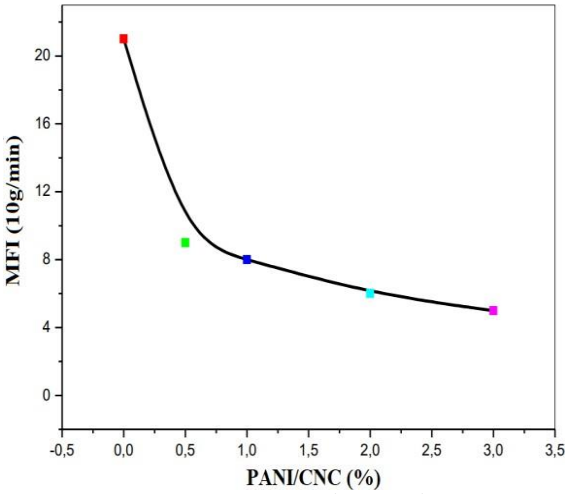

Figure 3. Fluidity index evolution as a function of PANI-CNC loading rate

By analyzing the obtained results, it is clear that PP's MFI (MFI= 21, more fluid) is very high compared to PP/PANI-CNC nanocomposite materials. The index fluidity decreases as a function of charge rate, molar mass (MW) increases by particles or aggregates presence of PANI-CNC. Fluidity decreases rapidly at a low rate (0.5%) then gradually, from this concentration. These results indicate that at a low rate, PANI-CNC particles are well dispersed and however, present obstacles to the flow at high loading rates [30].

E. Mechanical characterization:

Variations in mechanical properties (Young modulus (E), elongation at break and tensile strength at break) of PP/PANI-CNC nanocomposites as a function of PANI-CNC loading rate are represented in the Figures 4.

(a) **(b)**

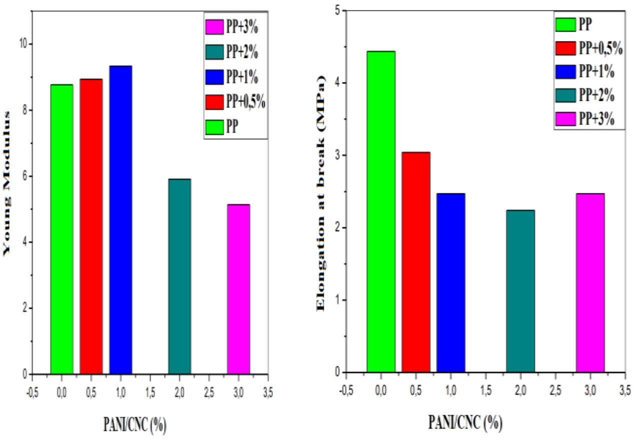

(c)

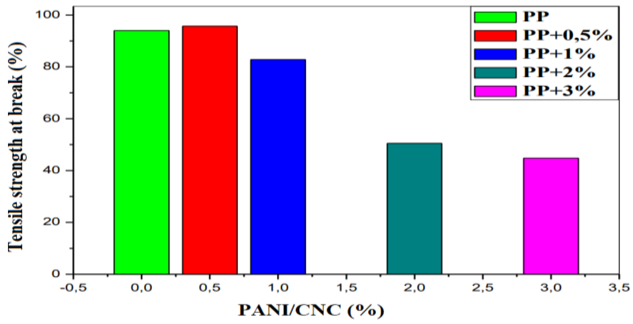

Figure 4. Tensile properties of PP/PANI-CNC nanocomposites: (a) Young's modulus, (b) Elongation at break, (c) Tensile strength at break

The above figures reveal that adding PANI-CNC particles increase slightly the Young modulus from 7.96 GP for pure PP to an Emax of 9.33 GP for PP at 1% loading rate.

With the addition of 0.5% by weight of PANI-CNC, nanocomposite tensile strength improved from 94 MPa for pure PP to 95.7 MPa, with a simultaneous decrease in elongation at break from 4.43% to 3.04%.

When CNC content exceeds 0.5% by weight, tensile strength and elongation at break gradually decreases while the Young's modulus has greatly increased (PP-PANI-CNC 1%). When PANI-CNC content exceeds 1% by weight, tensile strength, elongation at break and Young's modulus decrease gradually while with 3% of PANI-CNC, there is an increase in elongation at the break.

Composites mechanical properties are profoundly influenced by their composition and morphology [26], Fraysse et al [31], who carried out thermomechanical studies on PMMA/PANI composites and reported that PMMA mechanical behaviors is not modified with PANI addition for percentages of up to 0.5% by weight, while a sudden change is recorded above 1% concentration of PANI.

It has been reported that PANI addition to conventional polymers above the percolation threshold don't alters their mechanical properties because the conductive phase is dispersed in the form of separate islands in the continuous polymer matrix and it does not have a significant influence on composite macroscopic properties, therefore, while for CNC rates above the percolation threshold, the crystal structure of the polymer matrix alters and mechanical properties decrease [26,32].

These results indicate that a concentration at 0.5 and 1% is an adequate concentration for optimal distribution of PANI/CNC particles, since it has an improvement in the Young modulus and a better toughness by reducing elongation at break. Maleated coupling agents proved their efficiency in improving interfacial bonding between CNC's hydroxyl groups and hydrophobic polymers as PP [33]. This improvement confirms that PP-g-MA contributed in developing an interconnected structure from PP matrix and CNCs which are not covered by PANI through the reaction of MA groups and CNC's hydroxyls groups and anchoring of the PP compatibilizer chains into the PP phase leading to an efficient stress transfer between these components. Accordingly, it is reported that improvement of uniaxial traction properties is due to the homogeneous distribution of CNCs in PP matrix and bonds formation with the compatibilizer [34,35].

Izod impact tests were carried out as a function of PANI-CNC mass percentage and represented in Figure 5.

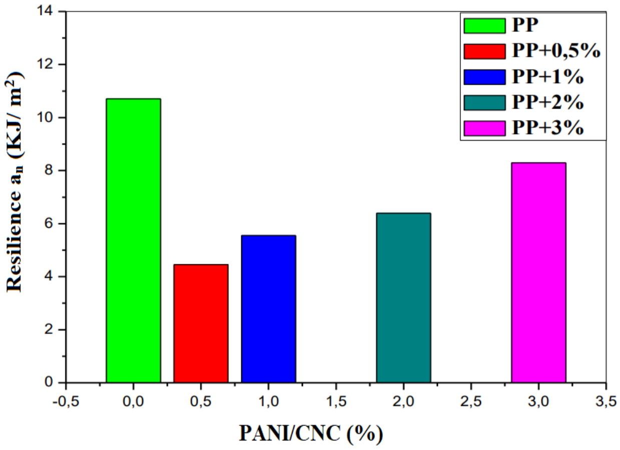

Figure 5. Variations of impact strength for PP/PANI-CNC nanocomposites versus PANI-CNC content

Figure 5 shows the impact resistance evolution; we observed a drop in PP resilience with a load rate at 0.5% of PANI-CNC which agree with the tensile results. Above this concentration, a slight improvement in impact resistance is observed.

Conclusion

In the present paper, cellulose nanocrystals CNC were incorporated into a polypropylene PP matrix for the development of improved nanocomposites. For this, Polyaniline was synthesized by oxidative polymerization in the presence of CNCs in suspension as support for CNCs optimal distribution. PANI-CNC blend was incorporated into PP matrix. PP-grafted maleic anhydride was used to develop interactions between non-PANI-related CNCs with PP.

Characterization by measuring conductivity by a multimeter confirmed the conductive nature of the PANI/CNC composites and therefore of the synthesized Polyaniline. Conductivity measurement is in the high range of semiconductors.

FTIR characterization shows that PANI was polymerized on cellulose nanocrystals surface illustrated by appearance of CNC's and PANI characteristic peaks in the infrared spectrum of PANI/CNC composites. AFM results also showed that PANI covered the CNCs.

PP/PANI-CNC nanocomposites development was carried out by melt mixing. Mechanical characterization of composites based on PP loaded with PANI/CNC particles shows an improvement in mechanical performance of these nanocomposites, this improvement is due to the particles good dispersion within the matrix, especially at low loading rates 0.5 to 1%.

We observe a drop in resilience with a CNC-PANI loading rate of 0.5%, which is in agreement with tensile results, a progressive improvement up to 3%, this is due to the particles morphology, their dispersion, their orientation and interactions.

Electrical characterization carried out by the four-point method on the composite materials shows that the produced films have a low conductivity and the highest value is noted on the nanocomposites with 2% PANI-CNC. However, the resulting composites did not achieve the conduction levels shown by PANI-CNC blend alone.

At high PANI-CNC loading rates, it tend to agglomerate into aggregates.

Acknowledgment

The author(s) received no financial support for the research, authorship, and/or publication of this article.

Conflict and interest

The author(s) declared no potential conflicts of interest with respect to the research, authorship, and/or publication of this article.

References.

[1] J. He, N. Li, K. Bian, G. Piao. Optically active polyaniline film based on cellulose nanocrystal. Carbohydrate Polymers 208, 398-403, 2019

[2] K. Jedvert, T. Heinze. Cellulose modification and shaping – a review. Journal of Polymer Engineering 37, pp 1-16, 2017.

[3] A. Dufresne. Cellulose nanomaterial reinforced polymer nanocomposites. Current Opinion in Colloid & Interface Science 29, 1–8, 2017.

[4] H. An, W. Ying, X. Wang, L. Na, L. Zheng. The preparation of PANI/CA composite electrode material for supercapacitors and its electrochemical performance. Journal of Solid State Electrochemistry 14, 651-657, 2010.

[5] Y. Habibi, L.A. Lucia, O.J. Rojas. Cellulose Nanocrystals: Chemistry, Self-Assembly, and Applications. Chemical Reviews 110, 3479-3500, 2010.

[6] M. Kılıç, Ü. Alkan, Y. Karabul, H. B. Yamak, O. İçelli. The Effects of PANI Concentration on the Mechanical Properties of PP/PANI Composites. Afyon Kocatepe University Journal of Science and Engineering 18, 426-433, 2018.

[7] D. Byelov, P. Panine, W. H. de Jeu. Shear-Induced Smectic Order in Isotactic Polypropylene Revisited. Macromolecules 40, 288–289, 2007.

[8] J.S. Kim, D.H. Kim. Compatibilizing effects of maleic anhydride-grafted-polypropylene (PP) on long Carbon fiber-reinforced PP composites. Journal of Thermoplastic Composite Materials 28, 1599–1611, 2015.

[9] J.Z. Liang, T.Y. Zhou, S.Y. Zou. Non-isothermal crystallization properties of polypropylene composites filled with multi-walled carbon nanotubes. Polymer Testing 55, 184–189, 2016.

[10] X. Wang, J. Liu, S. Zhang, D. Chimin. Flexible conductive polyaniline-silica/polypropylene composite membrane. Synthetic Metals 162, 1459–1463, 2012.

[11] A. Ameli, P.U. Jung, C.B. Park. Electrical properties and electromagnetic interference shielding effectiveness of polypropylene/carbon fiber composite foams. Carbon 60, 379–391, 2013.

[12] Zh. A. Boeva, V.G. Sergeyev. Polyaniline: Synthesis, Properties, and Application. Polymer Science Series C 56, 144–153, 2014.

[13] S.I. Abd Razak, W.A.W. Abdul Rahman, S. Hashim, M.Y. Yahya. Polyaniline and their Conductive Polymer Blends: A Short Review. Malaysian Journal of Fundamental and Applied Sciences 9, 74–80, 2013.

[14] S. Piletsky, E. Piletska, A. Bossi, N. Turner, A. Turner. Surface Functionalization of Porous Polypropylene Membranes with Polyaniline for Protein Immobilization. Biotechnology and Bioengineering 82, 86-92, 2003.

[15] S. Zhang, G. Sun, Y. He, R. Fu, Y. Gu, Sh. Chen, Preparation, Characterization, and Electrochromic Properties of Nanocellulose-Based Polyaniline Nanocomposite Films, ACS Appl. Mater. Interfaces 9, 16426−16434, 2017.

[16] A. Chiolerio, S. Bocchini, M. Crepaldi, K. Bejtka, C. F. Pirri. Bridging Electrochemical and Electron Devices: Fast Resistive Switching Based on Polyaniline from One Pot Synthesis Using FeCl3 as Oxidant and Co-Doping Agent. Synthetic Meterials 229, 72-81, 2017.

[17] N. D. Luong, J. T. Korhonen, A.J. Soininen, J. Ruokolainen, L.S. Johansson, J. Seppälä. Processable Polyaniline Suspensions Through in Situ Polymerization onto Nanocellulose. European Polymer Journal 49, 335-344, 2013.

[18] W. He, J. Tian, H. Jin, Y. Li. Characterization and Properties of Cellulose Nanofiber/Polyaniline Film Composites Synthesized through in Situ Polymerization. Bioresources 11, 8535- 8547, 2016.

[19] A.L. Goffin, J.M. Raquez, E. Duquesne, G. Siqueira, Y. Habibi, A. Dufresne, Ph. Dubois. From interfacial ring opening polymerization to melt processing of cellulose nanowhisker-filled polylactide-based nanocomposites. Biomacromolecules 12, 2456–2465, 2011.

[20] A.L. Goffin, J.M. Raquez, E. Duquesne G. Siqueira, Y. Habibi, A. Dufresne, Ph. Dubois. Poly(ε-caprolactone) based nanocomposites reinforced by surface-grafted cellulose nanowhiskers via extrusion processing: morphology, rheology, and thermo-mechanical properties. Polymer 52, 1532–1538, 2011.

[21] J.M. Raquez, Y. Murena, A.L. Goffin, Y. Habibi , B. Ruelle, F. DeBuyl, Ph. Dubois. Surface-modification of cellulose nanowhiskers and their use as nanoreinforcers into polylactide: a sustainably-integrated approach. Composites Science and Technology 72, 544–549, 2012.

[22] X. Ma, Y. Wang, Y. Shen, J. Huang, A. Dufresne. Current Status of Nanocellulose-Based Nanocomposites. In Jin Huang, Alain Dufresne, and Ning Lin (Eds), Nanocellulose, Inc, Wiley-VCH Verlag GmbH & Co. KGaA, 155–200, 2019.

[23] L. Benchikh, A. Merzouki, Y. Grohens, M. Guessoum, I. Pillin. Characterization of cellulose nanocrystals extracted from El Diss and El Retma local plants and their dispersion in poly(vinyl alcohol-co-ethylene) matrix in the presence of borax. Polymers and Polymer Composites 29, 218-230, 2021.

[24] D. Zhang, L. Zhang, B. Wang and G. Piao. Nanocomposites of Polyaniline and Cellulose Nanocrystals Prepared in Lyotropic Chiral Nematic Liquid Crystals. Journal of Materials, 1-6, 2013.

[25] S. Zhang, G. Sun, Y. He, R. Fu, Y. Gu and S. Chen. Preparation, Characterization, and Electrochromic Properties of Nanocellulose-Based Polyaniline Nanocomposite Films. ACS Appl. Mater. Interfaces 19, 16426-16434, 2017.

[26] U.M. Casado, M.I. Aranguren, N.E. Marcovich. Preparation and characterization of conductive nanostructured particles based on polyaniline and cellulose nanofibers. Ultrasonics Sonochemistry 21, 1641-1648, 2014.

[27] J. A. Marins, B. G. Soares, K. Dahmouche, S. J. L. Ribeiro, H. Barud, D. Bonemer, Structure and properties of conducting bacterial cellulose-polyaniline nanocomposites. Cellulose 18, 1285-1294, 2011.

[28] L. Benchikh, Y. Aitferhat, M. Kebaili, H. Chorfi, I. Abacha , M. Guessoum, A. Merzougui, H. M. Benia, Y. Grohens. Acetylation of cellulose nanocrystals extracted from cotton for drilling fluid application: structural and thermal characterization. International Journal of Nanoscience 22, 2023.

[29] M. Cochet, W. K. Maser, A. M. Benito, M. A. Callejas, M. T. Martínez, J. M. Benoit, J. Schreiber, O. Chauvet. Synthesis of a new polyaniline/nanotube composite: “in-situ” polymerisation and charge transfer through site-selective interaction. Royal Society of Chemistry 16, 1450-1451, 2001.

[30] L. Benchikh, A. Merzouki, Y. Grohens, I. Pellin. Extruded poly(ethylene–co–vinyl alcohol) composite films reinforced with cellulosic fibers isolated from two local abundonates plants. Journal of Fundamental and Applied Sciences 12, 49-72, 2019.

[31] J. Fraysse, J. Planès, A. Dufresne, A. Guermache. Thermo mechanical Studies of Poly (aniline)/Poly (methyl methacrylate) Blends: Relationship with Conducting Properties. Macromolécules 34, 8143 - 81482001, 2001.

[32] J. Huang, P.R. Chang, Y.Chen, S.Gao and J. Lia. Fully Green Cellulose Nanocomposites. In H. Kargarzadeh, I. Ahmad, S. Thomas, and A. Dufresne (Eds), Handbook of Nanocellulose and Cellulose Nanocomposites, Wiley-VCH Verlag GmbH & Co, Inc, Germany; pp 918, 2017.

[33] M. E. González-López, J. R. Robledo-Ortíz, R. Manríquez-González, J. A. Silva-Guzmán, A. A. Pérez-Fonseca. Polylactic acid functionalization with maleic anhydride and its use as coupling agent in natural fiber biocomposites: a review. Composite Interfaces 25, 1–24, 2018.

[34] Z. Kassab, F. Aziz, H. Hannache, H.B. Youcef, M. El Achaby. Improved mechanical properties of k-carrageenan-based nanocomposite films reinforced with cellulose nanocrystals. International Journal of Biological Macromolecules 123, 1248-1256, 2018.

[35] M. Achaby, Z. Kassab, A. Barakat, A. Aboulkas. Alfa fibers as viable sustainable source for cellulose nanocrystals extraction: Application for improving the tensile properties of biopolymer nanocomposite films. Industrial Crops and Products 112, 499-510, 2018.

Evaluation of mechanical and physical properties HDPE/Coffee grounds composites with different filler particles size.

Nadira BELLILI[1,2*]; Badrina DAIRI[1,2]; Nadjia Rabehi[1]; Sara LARKEM[1].
[1]*Department of Process Engineering, Faculty of Technology, Skikda University 20 Aout – 1955 – Algeria*
[2]*Department of Process Engineering, Faculty of Technology, Laboratory of Advanced Polymer Materials (LMPA), Abderrahmane MIRA University, Béjaïa 06000, Algeria*
**Corresponding author email:* n.bellili@univ-skikda.dz *dina_1961s@yahoo.fr*

Received: 17 November, 2023; Accepted: 20 November, 2023; Published: 24 January, 2024.

Abstract

Plant-based fiber composites are currently experiencing strong growth due in particular to the growing interest in them from the automotive industry. These fibers present an excellent alternative to glass fibers from an environmental point of view due to their biodegradability and their much more neutral combustibility in terms of the release of harmful gases or solid residues. However, the incorporation of cellulosic materials in the thermoplastic matrix affects a large number of properties. Many factors such as the nature and size of the filler incorporated may influence the properties of composites.

This present work consists, to study the effect of the particle size of a natural waste on the mechanical and physical properties of a polymer matrix. Different formulations based on HDPE/ Coffee grounds flour were prepared with loading rate of 20 % and different sizes of coffee grounds flour particles (125, 180 and 250 µm). They were, characterized by mechanical tests using the tensile and the impact test. The Physical properties of composites are, obtained by the density measurement.

Keywords: *Mechanical properties, natural waste, physical treatment, polymer composites*

I. Introduction

As an alternative to metals and ceramics, polymer materials have the potential to reduce weight and enhance part performance polymer materials possess a wide range of distinctive properties that are beneficial in a diverse range of applications [1]. The dramatic increase in demand for produced products prompts the development of composite materials offering new opportunities for advanced technology [2]. Furthermore, industrial waste as natural fibers can be, used and reduced the fabrication expense of the polymer composites. Therefore, they can play a significant role to enhance their mechanical properties of the latter. Different types of reinforcement are, used with different ratios, and sizes to reveals, the influence of reinforcement on the physical and mechanical properties of polymer matrix composite material. Recently, industrial waste as filler particles with different sizes are widely used in polymer matrix composites and are extensively employed now a, days world, wide are in industrial applications. These industrial wastes used to improve physical, mechanical, thermal and wear resistance properties [3–5]. This present work consists of studying the effect of the particle size of coffee grounds on the mechanical and physical properties of HDPE/coffee grounds composites.

II. Material and methods

The HDPE 5502 type and coffee grounds flour (CGF) are, mixed until the mixture becomes homogeneous. Four formulations were prepared, the pure HDPE (formulations noted F0) and mixtures of 80% HDPE and 20% coffee grounds flour particles size of 250 µm (formulations noted F20/250 µm) , particles size of180 µm (formulations noted F20/180 µm) and particles size of 125 µm (formulations noted F20/125 µm) . The mixtures obtained are, mixed in a two-cylinder mixer (Calendrer). The rotation speed of the two cylinders is around 16 rpm at a temperature of 177°C for a residence time of 15 min. The leaves obtained were, cut into small strips of 2 to 3 cm in length then crushed into small particles. For the preparation of the specimens, the small pieces that have already been cut are put into molds to prepare plates using automatic hydraulic press under a pressure of 100 Kg/cm² at a temperature of 177°C and a time (preheating: 10 min, degassing: 1 min and compression: 7

min). The plates obtained were, cut into the appropriate shapes to characterize them.

The properties of the HDPE/CGF composites developed are then determined by the tensile test, the impact test and by measuring the density.

III. Results and discussion

A. Mechanical properties of HDPE/CGF composites determined by the tensile test

The effect of the particles size of coffee grounds flour (CGF) on the mechanical properties of HDPE/CGF composites was, studied and the results obtained are, illustrated in the figures 1, 2 and 3.

The stiffness of a material and its resistance to elastic deformation are, often represented by the Young's modulus, measured by the slope of the linear part of the stress/strain curve obtained by the tensile test. Figure 1 shows the evolution of the Young's modulus of HDPE/Coffee grounds flour composites at different filler particle sizes.

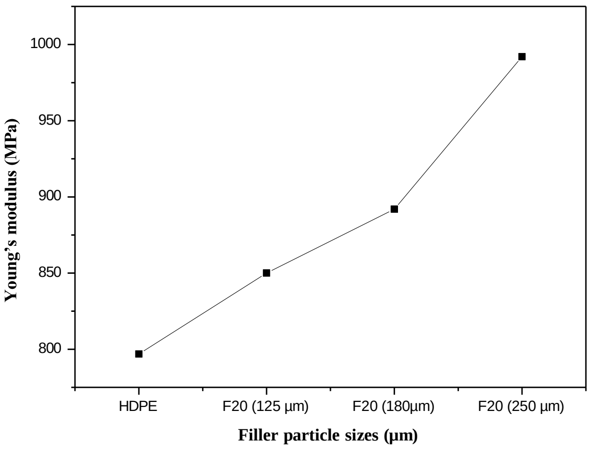

Figure 1. Evolution of the Young's modulus of HDPE/Coffee grounds flour composites at different filler particle sizes

The introduction of the filler into the HDPE matrix increases the rigidity of the material, and reduces their elasticity, which explains the increase in Young's modulus. In addition, the increase in the latter is all the more significant as the size of the CGF particles is high.

The results obtained are similar to those obtained by H. Djidjelli et al., for composites (PVC/olive pomace) and M. Kaci for low-density polyethylene/olive husk flour composites [6, 7].

This result highlights the reinforcing character played by the CGF, this could be, explained by the fact that the particles of the rigid character tend to form a reinforcement inside the composites leading to high resistance.

Figure 2 shows the evolution of the tensile stress at break of HDPE/Coffee grounds flour composites at different filler particle sizes.

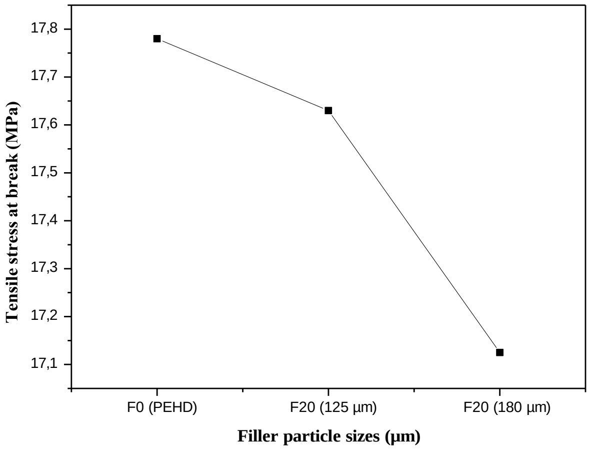

Figure 2. Evolution of the tensile stress at break of HDPE/Coffee grounds flour composites at different filler particle sizes

According to figure 2, one can clearly see a decrease in the breaking stress of the composites after incorporating the filler into the matrix and increasing the particle size of the coffee grounds filler.

This reduction is, attributed to the weak intefaciale adhesion between the filler and the polymer matrix and this is due to the fact that, the CGF particles gradually occupy a larger volume with a tendency to group together and agglomerate generating heterogeneities. They create defects in the polymer matrix consequently these areas of weakness reduce, the cohesion of the material, which is directly, linked to the filler/matrix interfacial adhesion.

Figure 3 shows the evolution of the tensile strain at break of HDPE/Coffee grounds flour composites at different filler particle sizes.

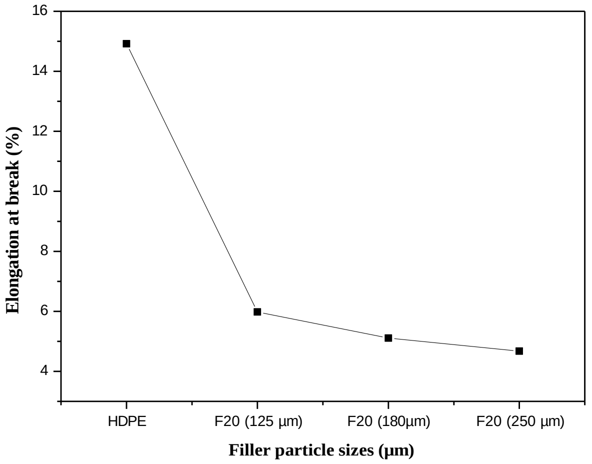

Figure 3. Evolution of the elongation at break of HDPE/Coffee grounds flour composites at different filler particle sizes

The incorporation of rigid coffee grounds filler into the HDPE matrix considerably reduces the mobility of the polymer chains and loses its flexibility, which accelerates the rupture of the specimens at low stresses, and this is, translated by a reduction in elongation at break, due to poor filler/matrix intefacial adhesion. The same observations were, made by Maldas D. et al. [8], Kamdem D. et al. [9] and Mulhaupt R. et al. [10].

B. The mechanical properties of composites obtained by the impact test

The resilience test (impact test) consists of breaking, with a single impact, a notched specimen and measuring the resilience R in (J/m2) absorbed by the break.
The impact resistance results are shown in Figure 4.

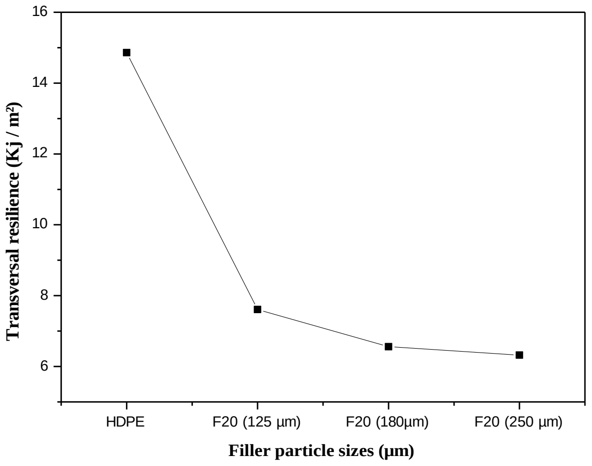

Figure 4. Evolution of the transverse resilience of HDPE/coffee grounds composites as a function of the particles size of the filler.

We find that the impact resilience of HDPE/coffee grounds composites decreases after the addition of the filler and with the increase in the size of the coffee grounds.
Coffee grounds flour, which has a greater rigidity than polyethylene, considerably increases the rigidity of the composite material, which also causes a reduction in impact resistance. This can be, attributed simply to the weak filler/matrix interfacial adhesion. The same observations were, made by Bendgtsson and Osman for composites (PE / Wood flour) [11].

C. Physical properties of composites obtained by the density measurement

The results obtained by measuring the density of the different samples are, summarized in table 1.

Table 1: Variation of HDPE/Coffee grounds flour composites density as a function of filler particle sizes

Samples	HDPE	F20 (125 µm)	F20 (180 µm)	F20 (250 µm)
Density (g/cm^3)	0.9555	>1	>1	>1

The density of composite depends, on CGF content and filler particle sizes. By the presence and increasing the filler particle sizes, the hydrophilicity of the composites will increase. The densities of HDPE and F20 composites at different filler particle sizes were from 0.95 up to greater than 1, respectively (Table I). The obtained data showed comparable results found by A. R. Oromiehie et al. [12].

IV. Conclusions

The objective of this work was to study the effect of the particle size of coffee grounds on the properties of HDPE/ coffee grounds composites. Three particle size classes were, studied: 250, 180 and 125µm. The composites obtained are, characterized by the determination of the mechanical and physical properties.
The analysis of the experimental results allowed us to draw the following main conclusions:

- ➢ The mechanical behavior of the HDPE/CGF composites shows that with the incorporation of 20% of CGF and with the increase in the particle size of the filler in the HDPE matrix, the impact resilience, tensile stress and elongation at break decreases, while the modulus of elasticity increases progressively.

- ➢ The density of HDPE/CGF composite increased by increasing the particle size of the filler in the HDPE matrix.

References.

[1] R. Yadav, M. Singh, D. Shekhawat, S-Y. Lee, S-J. Park., The role of fillers to enhance the mechanical, thermal, and wear characteristics of polymer composite materials. A review, Composites: Part A 175, 107775, 2023.

[2] R. Yadav, M. Kumar. Dental restorative composite materials. A review. Journal of Oral Biosciences 61(2):78–83, 2019.

[3] R. Yadav, M. Kumar. Investigation of the physical, mechanical and thermal properties of nano and microsized particulate-filled dental composite material, Journal of Composite Materials 54(19): 1–11, 2020.

[4] R. Yadav. Analytic hierarchy process-technique for order preference by similarity to ideal solution: A multi criteria decision-making technique to select the best dental restorative composite materials. Polymer Composite 42(12): 6867–6877, 2021.

[5] R. Yadav, A. Meena. Mechanical and two-body wear characterization of micro nano ceramic particulate reinforced dental restorative composite materials. Polymer Composite 43(1): 467–482.

[6] H. Djidjeli, A. Boukerrou, R. Founas, A. Rabouhi, M. Kaci, J. Farenc, J.J.J. Vega, D. Benachour. Thermal

dielectric and mechanical study of poly (vinyl chloride)/olive pomace composites. Journal of Applied Polymer Science 103: 3630-3636, 2007.

[7] M. Kaci, H. Djidjelli, A. Boukerrou, L. Zaidi, , Effect of wood filler treatment and EBAGMA compatibilizer on morphology and mechanical properties of low density polyethylene/olive husk flour composites. Express Polymer Letters 1 (7): 467–473, 2007.

[8] D. Maldas, B.V. Kokta, R.G. Raj, S.T. Sean. Use of wood fibers as reinforcing fillers for polystyrene. Materials Science and Engineering A104: 235-244, 1988.

[9] D. Kamdem, H. Jiang. Development of Poly (vinyl chloride)/Wood Composites. A Literature Review, Journal of vinyl and additive Technology. 10 (2): 59-69, 2004.

[10] R. Mulhaupt, F. Stricker, M. Bruch. Mechanical and thermal properties of syndiotactic polypropene filled with glass beads and talcum. Polymer 38 (21): 5347-5353, 1997.

[11] M. Bengtsson, P. Gatenholmand, K. Oksman. The Effect of Crosslinking on the Properties of Polyethylene/Wood Flour Composites. Composites Science and Technology. 65:1468-1479, 2005.

[12] A. R. Oromiehie, T. Taherzadeh lari., A. Rabiee. Physical and Thermal Mechanical Properties of Corn Starch/LDPE Composites. Journal of Applied Polymer Science 127 (2): 1128-1134, 2013.

[13] T. Masri, H. Ounis, L. Sedira, A Kaci., A. Benchabane. Characterization of new composite material based on date palm leaflets and expanded polystyrene wastes. Construction and Building Materials 164, 410-418, 2018.

Biopolymer Applications Journal **Badrina DAIRI et al.Vol 03. N°1, 2024, pp. 12-16**
e-ISSN : 2800-1729

Valorization of lignocellulosic fibers in the development of composite materials

Badrina DAIRI[1,2*], Nadira BELLILI[1,2], Wiam Djamila AYACHI[1], Ismahane NAKOUB[1], Sara LARKEM[1], Nadjia RABEHI[1] , Hocine Djidjelli [2]; Amar Boukerrou[2]

[1] Department of Process Engineering, Faculty of Technology, Skikda University 20 Aout – 1955 – Algeria;
[2] Department of Process Engineering, Faculty of Technology, Laboratory of Advanced Polymer Materials (LMPA), Abderrahmane MIRA University, Béjaïa 06000, Algeria;
**Corresponding author email: b.dairi@univ-skikda.dz*

Received: 22 November, 2023; Accepted: 22 December, 2023; Published: 26 January, 2024

Abstract

Natural fibers have recently attracted the attention of scientists because of their low-cost, low-density, renewable, biodegradable and non-abrasive properties. The growing use of composite materials is giving rise to problems of waste management. As a result, there is a growing trend towards the use of biodegradable products, either by using biodegradable polymers, or by incorporating biodegradable fibers into polymeric materials.

In this context, various high-density polyethylene-based formulations have been prepared (HDPE/Wood Flour, HDPE/Wheat Bran, and HDPE/Wood Flour/Wheat Bran).

The various composites were initially blended in a calender before the various samples, with average thicknesses of 2 and 3 mm, were prepared by compression at 190°C and characterized by mechanical test.

Keywords: *Wood flour, Wheat bran, Composite materials, High-density polyethylene.*

I. Introduction

In today’s world, the growing demand for more advanced materials has compelled humans to combine two or three different components to create new products with improved properties. The combination of components with complementary characteristics results in attractive and essential properties for specific applications. Materials obtained in this manner are called “composites,” and they currently represent a privileged area of scientific research [1,2].

One of the most significant advantages of polymers is their ease of processing, productivity, and cost reduction. For many applications, the properties of polymers are modified by using reinforcements and fillers [3].

The use of natural resources in composite materials is becoming increasingly common. Studies are dedicated to the valorization of lignocellulosic materials derived from wood and natural fibers as fillers in plastic matrices [4].

As a result, considerable attention in the research community is focused on the use of natural fibers as reinforcements in the design of composite materials, allowing for a combination of materials that are strong, lightweight, non-abrasive, structured, and cost-effective. However, despite these advantages, natural fibers present a major drawback when combined with plastics, especially polyolefins (such as polypropylene, polyethylene, polystyrene). Wood-based materials have a strong affinity for water (strongly hydrophilic character), which creates an interface incompatibility between lignocellulosic materials and highly hydrophobic thermoplastics. This interfacial incompatibility affects the synergy between the different constituents of the composite, knowing that the interface is the preferred location for stress transfer between the reinforcement and the matrix. To address this issue, many research efforts have been conducted to reduce the surface tension between plant fibers and thermoplastics [5].

The incorporation of cellulosic materials into high-density polyethylene matrices affects a wide range of properties. However, it has been found that the quality of adhesion alone does not dominate the properties of the composites, and other factors, such as the fraction, nature, or size of the incorporated filler, also come into play [6].

II. Material and methods

II.1 Raw Materials

The polymer used is high-density polyethylene of the type HDPE 5502. It is produced by the CP2K complex in Skikda and is marketed in the form of a white powder.

The WF was extracted from Aleppo pine trees, growing in the Djelfa region in the south of Algeria. The average particle size was approximately 63 µm.

Wheat bran is obtained after wheat grinding. Subsequently, all the grains are removed to retain only the bran. The wheat bran powder is processed to achieve a fine filler with a uniform particle size, with a diameter less than 63 µm (<63µm).

II.2 Preparation

The different formulations chosen for the preparation of our samples are provided in the following table:

Table 1 The mass compositions of the various formulations.

Compositions	HDPE (%mass)	Wood flour (% mass)	Wheat bran (% mass)
HDPE	100	0	0
HDPE/WF	80	20	0
HDPE/WB	80	0	20
HDPE/WF/WB	80	10	10

The pre-blends of HDPE/Wood Flour, HDPE/Wheat Bran, and HDPE/Wood Flour/Wheat Bran are prepared in a double-roll mixer (Calender) of the brand IQAP LAP at the "CP2K, Skikda" facility. The rotational speed of the two cylinders is approximately 32 rpm, and their temperature is set at 170°C. After 8 minutes, composite films with a thickness of 1mm are obtained.

After the mixing process, we obtained a mixture of HDPE/Wood Flour, HDPE/Wheat Bran and HDPE/Wood Flour/Wheat Bran, which we cut into small pieces (2 to 3 cm) using a manual cutter. These pieces are then placed in molds to create samples in the form of dumbbells and squares for subsequent use in various characterization tests.

The films obtained through calendering are cut into small pieces and then placed between two insulating Teflon sheets, which are interleaved between two metal plates in a hydraulic press. They are heated to a temperature of 190°C for a total dwell time of 15 minutes, with 7 minutes allocated for preheating and 8 minutes for compression and degassing.

Upon exiting the press, the samples are cooled in the open air and carefully removed from the mold. Various shapes of samples with a thickness of 3mm are obtained, which will be subjected to various characterizations.

III. Characterization

The measurement of mechanical properties at the point of rupture of the samples is conducted using a TesTGmbH tensile testing machine at room temperature. The samples are cut into dumbbell-shaped specimens of "H" type with dimensions of (92 x 13 x 3) mm³, following the ASTM D638 standard. The deformation rate is set at 20 mm/min.

Shore D hardness tests samples with a thickness of 6 mm are prepared using a press, and they are then placed beneath the needle. By operating the lever arm until the needle penetrates, three tests are conducted at different points, and then the average is calculated [7].

From a 3.17 mm thick plate, Izod impact test samples with dimensions L = 100 mm and l = 12.7 mm are prepared using a cutter. A central V-notch, 2.5 mm deep, is created on these samples. Three tests are conducted and the average value is recorded [7].

Morphological Characterization by Optical Microscopy to study the material's morphology and verify the dispersion of fibers in composite materials, optical microscopy is used to capture surface images of the obtained films. The equipment used is an optical microscope from OPTIKA Microscopes ITALY.

IV. Results and discussion

IV.1 Impact strength IZOD

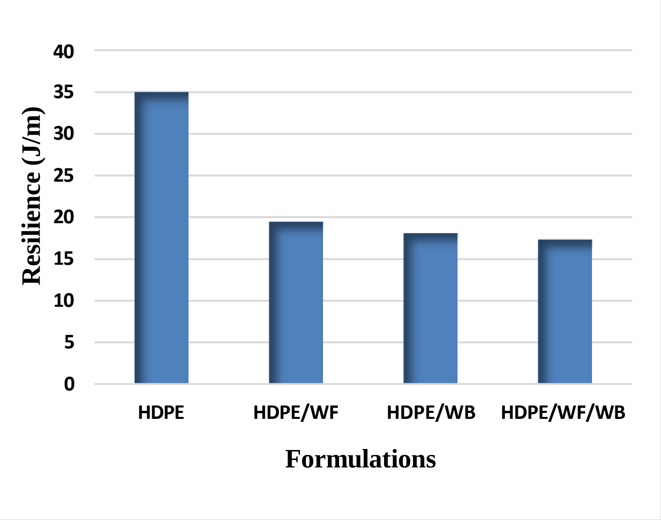

Figure 1. Evolution of the resilience of different composites developed with HDPE/Wood Flour, HDPE/Wheat Bran, and HDPE/Wood Flour/Wheat Bran.

According to figure 1, which illustrates the variations in the resilience of the HDPE/WF, HDPE/WB and HDPE/WF/WB composites, there is a clear decrease in impact resistance after the incorporation of Wood Flour and Wheat Bran into the HDPE matrix. This decrease is due to the increased rigidity and interfacial phenomena.

The HDPE/WF and HDPE/WB composites exhibit lower impact resistance values compared to pure HDPE. This indicates that wood flour and wheat bran have higher rigidity than high-density polyethylene, significantly increasing the composite material's rigidity, which, in turn, results in reduced impact resistance. This decline in impact resilience is also attributed to weak interactions (physical interactions) between the matrix and the filler, indicating poor interfacial adhesion. This has been previously confirmed by the work of Andrzej K. Bledzki et al and Ajay Karmarkar et al [8, 9].

IV.2 Shore D hardness test

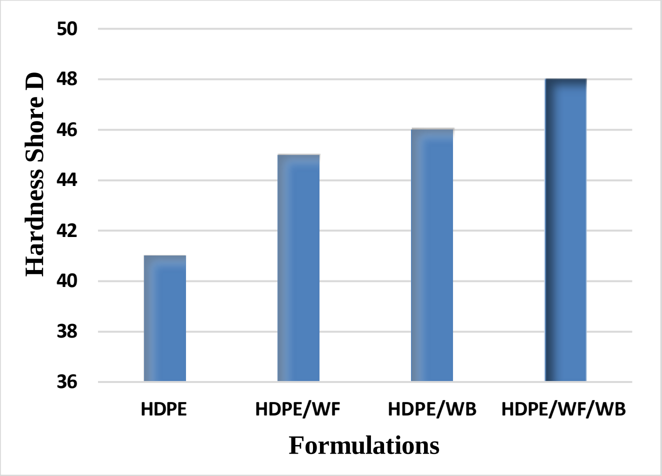

Figure 2. Evolution of the Shore D hardness of different composites developed with HDPE/Wood Flour, HDPE/Wheat Bran, and HDPE/Wood Flour/Wheat Bran.

According to figure 2, there is an increase in hardness with the incorporation of two types of fillers (Wood Flour and Wheat Bran) into the HDPE matrix. This increase is particularly significant for the hybrid composite (HDPE/Wood Flour/Wheat Bran).
These results are expected because the fillers consist of microcellulose fibrils, which are classified among hard fibers, making it more challenging for the durometer needle to penetrate the composite material. This outcome has been confirmed by Md. Rezaur Rabman et al and S. Th. Georgopoulos et al [10, 11].

IV.3 Tensile Test

IV.3.1 The evolution of tensile strength

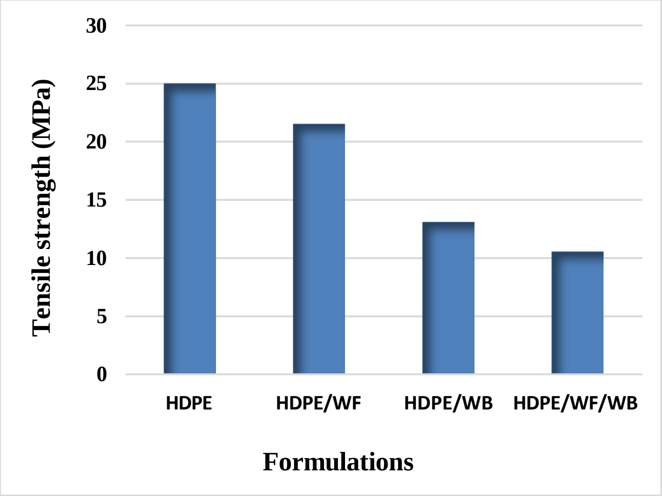

Figure 3. Evolution of the tensile strength of different formulations: HDPE, HDPE/Wood Flour, HDPE/Wheat Bran, and HDPE/Wood Flour/Wheat Bran.

A decrease in the breaking strength is observed for the various composites loaded with wood flour, wheat bran flour, and wood-wheat bran flour compared to the unloaded HDPE. These results are predictable and are in accordance with the findings of NM. Stark and R. E. Rowlands [12], B. Sanschagrin [13] and J. Simonsen [14]. They attributed this decrease to the reduction in the bond strength between the fillers and the matrix, which obstructs the transfer of stress and leads to a tendency to cluster together, forming agglomerates that induce heterogeneities and non-uniform stress transfer within the matrix, consequently resulting in a weakening of the composite material. In addition, there is a low interfacial adhesion between HDPE/Wood Flour, HDPE/Wheat Bran, and HDPE/Wood Flour/Wheat Bran due to the antagonistic nature (HDPE matrix being hydrophobic, while WF and WB fillers are hydrophilic). These results are consistent with those presented by K. Oksman and C. Clemons [15].

IV.3.2 Evolution of the Young's Modulus

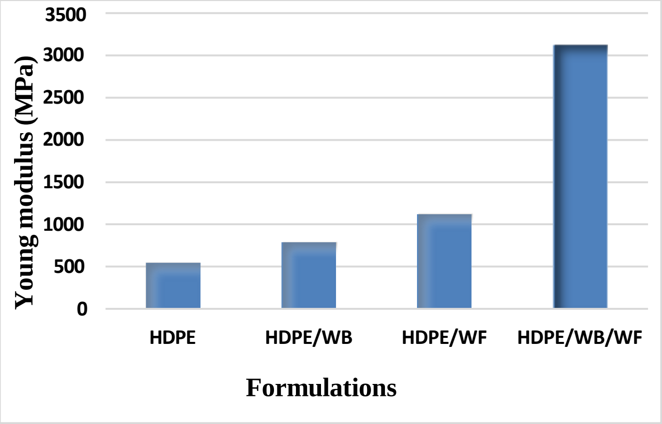

Figure 4. Evolution of the Young's Modulus of different formulations: HDPE, HDPE/Wood Flour, HDPE/Wheat Bran, and HDPE/Wood Flour/Wheat Bran.

The introduction of wood flour, wheat bran flour, and wood-wheat bran flour into the HDPE matrix increases the material's rigidity and reduces its elasticity. In other words, the Young's Modulus increases, and this increase is even more significant for the hybrid composite HDPE/Wood Flour/Wheat Bran. This can be explained by the fact that the rigid particles of wood flour and wheat bran flour tend to form a reinforcement within the composites, leading to greater strength. This is what NM. Stark and R. E. Rowlands [12] observed.

IV.3.3 Evolution of the elongation at break

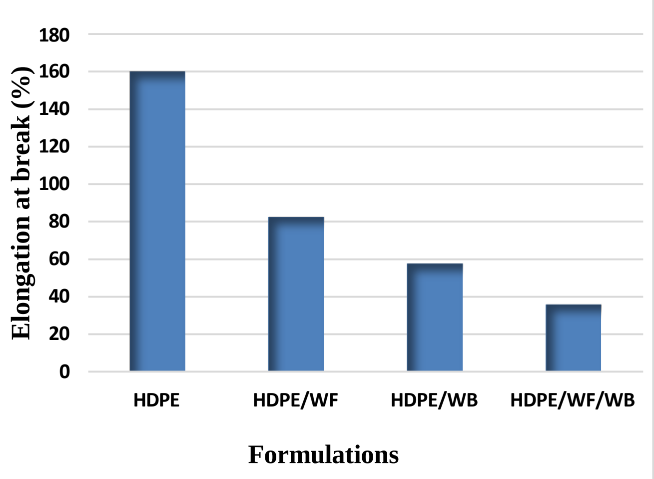

Figure 5. Evolution of the elongation at break of different formulations: HDPE, HDPE/Wood Flour, HDPE/Wheat Bran, and HDPE/Wood Flour/Wheat Bran.

There is a decrease in the elongation at break for the HDPE/Wood Flour and HDPE/Wheat Bran composites when compared to that of virgin HDPE, and this decrease is more significant for the hybrid composite HDPE/Wood Flour/Wheat Bran. This observation is in perfect agreement with many authors, such as B. A. Acha et al [16], T. T. L. Doan et al [17], S. J. Kim et al [18]. The deterioration of this property is primarily due to the incorporation of rigid wood flour and wheat bran flour into the HDPE matrix, which reduces the mobility of the polymer chains, leading to the premature failure of test specimens at low stresses.

IV.4. Morphology Analysis by Optical Microscopy

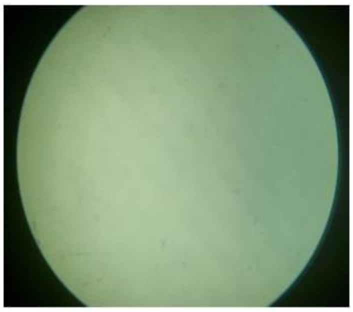

Figure 6. Optical microscopy micrograph of the surface of virgin HDPE.

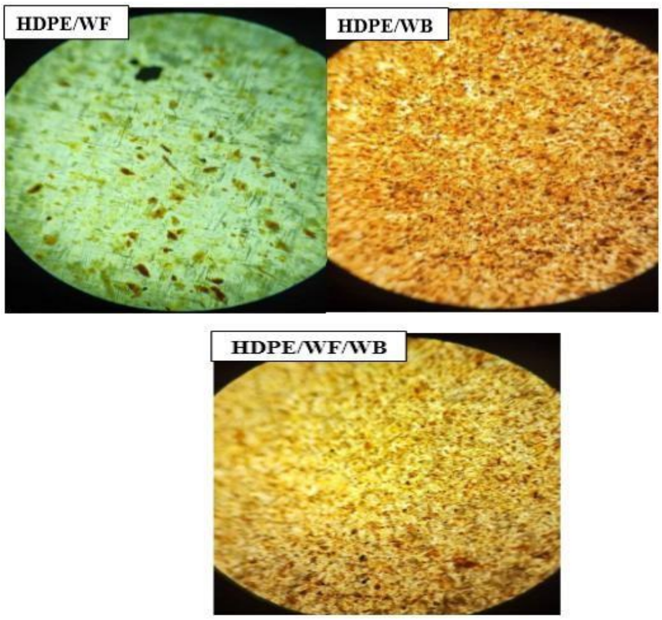

Figure 7. Optical microscopy micrograph of the surfaces of HDPE/Wood Flour, HDPE/Wheat Bran, and HDPE/Wood Flour/Wheat Bran composites.

The micrographs of the composites in figure 5 concerning the incorporation of wood flour, wheat bran flour and wood flour-wheat bran flour into the HDPE matrix, clearly depict a heterogeneous and irregular surface with the presence of aggregates that are completely separated from the high-density polyethylene matrix.

These aggregates increase in number in the hybrid composite HDPE/Wood Flour/Wheat Bran. This is due to the incompatibility of the two phases because of the low interfacial adhesion between wood flour and wheat bran flour, which have a hydrophilic nature and HDPE, which is hydrophobic.

V. Conclusions

The analysis of the experimental results has allowed us to draw the following main conclusions:

- The mechanical characterization of the developed composites has allowed for the deduction that:
  - ✓ He hardness of the developed composites HDPE/Wood Flour/Wheat Bran, is higher than that of virgin HDPE.
  - ✓ The resilience of the different developed composites HDPE/Wood Flour/Wheat Bran has decreased compared to that of virgin HDPE.
  - ✓ The mechanical behavior of the HDPE/Wood Flour/wheat Bran composites shows that both stress and elongation at the rupture decrease while the elasticity modulus increases progressively.
- The morphological characterization through optical microscopy of the HDPE matrix shows a homogeneous and regular surface, unlike the HDPE/Wood Flour, HDPE/Wheat Bran, and HDPE/Wood Flour/Wheat Bran composites, which clearly exhibit a heterogeneous and irregular surface with the presence of aggregates.

References.

[1] S. Nekkaa, M. Guessoum, N. Haddaoui, Water Absorption Behavior and Impact Properties of Spartium Junceum Fiber Composites, International Journal, 58, 468- 481, (2009).

[2] H. KIM, J. Biswas, S. Choe, Effects of stearic acid coating on zeolite in LDPE, LLDPE, and HDPE composites », South Korea Polymer, 47, 3981- 3992, (2006).

[3] A.B.M. Supian, M. Jawaid, B. Rashid, H. Fouad, N. Saba, H.N. Dhakal, R. Khiari, Mechanical and physical performance of date palm/bamboo fibre reinforced epoxy hybrid composites. J. Mater. Res. Technol, 15, 1330–1341, (2021).

[4] S.N.A. Safri, M.T.H. Sultan, M. Jawaid, K. Jayakrishna, Impact behaviour of hybrid composites for structural applications: a review, Compos. B, 133, 112–121, (2018).

[5] K. Ben Hamou, H. Kaddami, F. Elisabete, F. Erchiqui, Synergistic association of wood /hemp fibers reinforcements on mechanical, physical and thermal properties of polypropylene-based hybrid composites, Industrial Crops & Products, 192 116052, (2023).

[6] D. N. Saheb, J. P. Jog, Natural fiber polymer composites : a review, Advances in Polymer Technology, 18, 351–363, (1999).

[7] M. Abdellah, M.G. Sadek, H. Alharthi, G.T. Abdel-Jaber, Ahmed H. Backar, Characteristic properties of date-palm fibre/sheep wool reinforced polyester composites, Journal of Bioresources and Bioproducts, 8, 430–443, (2023).

[8] K.. Bledzki, O. Faruk, Creep and impact properties of wood fibre/polypropylene composites : influence of température and moisture content, Composites Science and Technology, 64, 693-700, (2004).

[9] A. Karmarkar, S.Chauhan, J. ayant, M. Modak, M. Chanda, Mechanical properties of wood -fîber reinforced polypropylene composites : Effect of a nevel compatibilizer with isocyanate fimctional group, Composites Part A, 38, 227-233, (2007).

[10] Md. R. Rahman, Md. M. Huque, Md. N. Islam, M. Hasan, Mechanical properties of polypropylene composites reinforced with chemically treated abaca, Composites Part A, 40, 511-517, (2009).

[11] S.Th.Georgopoulos, P.A.Tarantili, E.Avgerinos, A.G. Andreopoulos, E.G. Koukios, Thermopiastic polymers reinforced with fibrous agricultural residues, Polymer Degradation and Stability, 90, 303-312, (2005).

[12] N.Stark, R.E.Rowlands, Effects of wood fiber characteristics on mechanical properties of wood/polypropylene composites, Wood and fiber science, 35, 167- 174, (2003).

[13] B. Sanschagrin, S. T. Sean, B. V. Kokta, Mechanical properties of cellulose fibers reinforced thermoplastics, Proceedings of the 43rd annual conference, composite institute. Cincinnati, OH, États-Unis, 1-5 février, (1988).

[14] J. Simonsen, Effiency of reinforcing materials in filled polymer composites, Forest Products Society, 47, 74-81, (1997).

[15] K.Oksman, C.Clemons, Mechanical properties and morphology of impact modified polypropylene-wood flour composites, J. App. Polym. Sci, 67, 1503- 1513, (1998).

[16] B. A. Acha, M. M. Reboredo, N. E. Marcovich, Effect of coupling agents on the thermal and mechanical properties of polypropylene–jute fabric composites, Polym. Inter, 55, 1104–1113, (2006).

[17] T. T. L. Doan And All, Jute /PP composites, Effect of matrix modification , Compos. Sci. Tech, 66, 952-963, (2006).

[18] S.J.Kim, J.B.Moon, G.H.Kim, C.S.Ha, Mechanical properties of polypropylene/natural fiber composites, comparison of wood fiber and cotton fiber, Polym. Testing, 27, 801-806, (2008).

Biopolymer Applications Journal **Naima BRINIS et al. Vol 03. N°1, 2024, pp. 17-20**
e-ISSN : 2800-1729

Anticorrosive performance of MoO_4^{-2}-doped polyaniline conductive polymer

Naima BRINIS*; Kahina ABDOUNE; Kahina AOUDIA; Hassiba TIGHIDET; Nabila CHERCHOUR
Laboratoire d'Electrochimie, Corrosion et de Valorisation Energétique, Faculté de Technologie, Université A. MIRA de Béjaïa, Béjaïa (06000), Algeria
**Corresponding author email: naima brinis@univ-bejaia.dz*

Received: 24 November, 2023; Accepted: 22 December, 2023 ; Published : 27 January, 2024

Abstract

Electrodeposition polyaniline (PANI) and polyaniline doped (PANI-MoO_4^{-2}) coatings on steel was prepared in oxalic acid solution by potentiodynamic polarization technique. Morphology of the surface coatings was analyzed by scanning electron microscopy (SEM). The protective properties and electrochemical behavior of such coatings in 0.5MH_2SO_4 pH0.3 solution were investigated using open-circuit potential versus time of exposure and electrochemical impedance spectroscopy (EIS). It was shown that PANI coating presented an anodic protection and their doping by molybdate ions increased considerably the protection time.

Keywords: *Anodic protection, Corrosion, Polyaniline, Sodium molybdate, Steel.*

I. Introduction

The protection of mild steels against corrosion by a layer of conductive polymer CP has gained significant attention in recent years. Conductive polymers such as polyaniline (PANI), polypyrrole (PPy), and polythiophene (PTh) have been studied for their potential in providing corrosion protection to mild steel [1-5]. Research literature has demonstrated a noticeable enhancement of protection of ferrous materials against corrosion using conducting polymers as coatings, making them an ideal potential for corrosion protection of mild steel and other ferrous alloys. These CP produce a galvanic effect characterized as anodic protection, where the oxidizing power of the CP is capable of setting the metal in a passive state. This has been particularly observed in the case of iron and ferrous metals [3, 6].

The electropolymerization of aniline has been the subject of numerous studies since its first use in 1985, when DeBerry showed that the PANI deposited electrochemically reduced significant the rate of corrosion of steel in acidic environment [7]. These coatings can be applied individually or as a primer layer in a coating system [8]. Research has shown that the addition of dopants can influence the corrosion protection behavior of polyaniline coatings on metals such as mild steel [9] and 304 stainless steel [10]. The influence of molybdate ion dopants in corrosion protection behavior of polyaniline coating on mild steel has been investigated, and it was found that the dopants can affect the long-time corrosion resistance of the coated metal [11].

Different protection mechanisms of polyaniline (PANI) coatings have been proposed, including anodic protection, barrier protection, corrosion inhibition, and the shift of the electrochemical interface. Studies have shown evidence of the anodic protection of PANI coatings, as indicated by the shift in the corrosion potential to the passive region and an increase in the polarization resistance for the metal [10].

In this work, a description of the synthesis conditions of doped PANI-MoO_4^{-2} and non-doped PANI coatings and corrosion tests in H_2SO_4 pH0.3 will be reported.

II. Material and methods

PANI (ANI from PanReac AppliChem, purity 99 %) coatings were deposited on the pretreated steel surface at the potential 300 V/SSE in oxalic acid solution ($C_2H_2O_4$) containing 0.1 M of aniline. The various concentrations of ions (MoO_4^{-2}) are added to the synthesis medium in the form of sodium molybdate Na_2MoO_4 (from Fluka, purity 99 %). Oxygen bubbles evolved at the beginning of the process during synthesis and by consequent, a rotating disk electrodes was necessary for remove it.

All electrochemical experiments were carried out at room temperature (θ = 25 ± 0.1°C) with a three electrode cell arrangement; a counter electrode made of a large platinum grid, a working electrode (steel, Φ = 10 mm) and a sulfate reference electrode in saturated K_2SO_4 solution (SSE).

Before each measurement, the exposed area of the working electrode was polished and washed with double deionized water to ensure the same initial surface state.

Corrosive tests were carried out in 0.5M H_2SO_4 solutions with OCP versus time of exposure and electrochemical impedance spectroscopy (EIS).

The morphology and the elemental composition of the PANI and PANI-MoO_4^{-2} coatings was examined with FEI Quanta 200 Scanning electron microscope (SEM) coupled with an Isis X-Ray analysis system energy dispersive X-rays (EDX).

III. Results and discussion

A. Influence of electrolyte concentration

As we know, the electrodeposition of polymers on steel surface directly is difficult, the formation of a passive layer is required [12, 13]. Based on the search results and after preliminary experiments [8, 14], a potentiostatic electropolymerization at 300 mV/ SSE was chosen.

We have tested several electrolyt at different concentrations (oxalic acide, phosphoric acide, sulfuric acide) and the best result after the corrosion test is obtained in oxalic acid medium at different concentrations as shown in figure 1. After synthesis, PANI coatings are rinsed with distilled water, dried and then immersed in H_2SO_4 0.5M (pH 0.3).

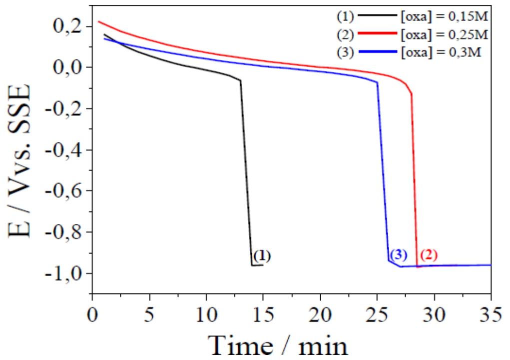

Figure 1. OCP curve versus time in H_2SO_4 pH 0.5 solution for PANI-coated steel polymerized at different oxalic acid concentrations. Synthesis time = 6 hours. i = 2 mA.cm^{-2}

The sudden drop in potential is used to estimate the time t_c at which the PANI coating loses its protective properties. However, after this drop, the PANI coating still provides some protection to the steel substrate through a simple polymer barrier effect. It is important to note that this effect is not taken into consideration when estimating the time of loss of protection [15].

According to figure 1, all the curves have the same starting with a positive potential but show different protection times. The PANI layer synthesized in 0.25M oxalic acid shows a longer protection time, this result is linked to the quality of the film under these synthesis conditions, which provides galvanic anodic protection [8].

B. Influence of synthesis time

Figure 2 shows the corrosion test results obtained on PANI films at different synthesis times.

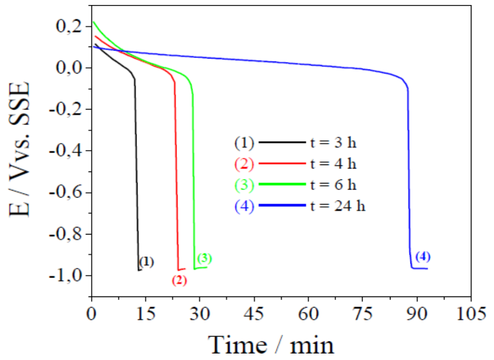

Figure 2. OCP curve versus time in H_2SO_4 pH 0.5 solution for PANI-coated steel polymerized in 0.25M oxalic acid at different synthesis times.
i = 2 mA.cm^{-2}

It is noted that the protective effectiveness of the steel increases proportionally with the synthesis time of PANI films. This result is linked to the thickness of film formed and to quantity of electric charge available (see Table 1) that the film can deliver to ensure galvanic anodic protection. The thickness of the layer has considerable effects on the corrosion behavior of steel.

Table 1. Quantity of electricity consumed Qp for current density i = 2 mA.cm-2 at different synthesis times.

Synthesis time (h)	**3**	**4**	**6**	**24**
Q_p (mC.cm^{-2})	316	547	556	2122
Protection time (min)	12	24	28	88

The SEM analysis of the formed film at 6h of synthesis shows a uniform and homogeneous deposit, as shown in figure 3 (A). After 30 minutes immersion in H_2SO_4 pH0.3 (figure 3 (B)), we notice attacks depths of the coating translated by the development of lesions on the surface, leaving thus steel in its bare state.

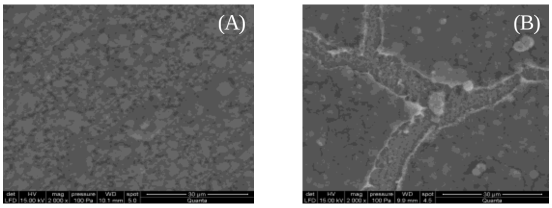

Figure 3. SEM picture of PANI-coated steel polymerized in 0.25M oxalic acid solution : (A) before and (B) after 30 min immersion in H_2SO_4 pH0.3

EIS studies

Electrochemical Impedance Spectroscopy (EIS) was used as a powerful complementary method to obtain additional information about the corrosion inhibition properties of PANI coatings. The impedance response represented on Nyquist diagram of PANI coating as a function of the immersion time in H_2SO_4 solution at 0.5 M is presented in figure 4. The synthesized time of the films is 6 hours.

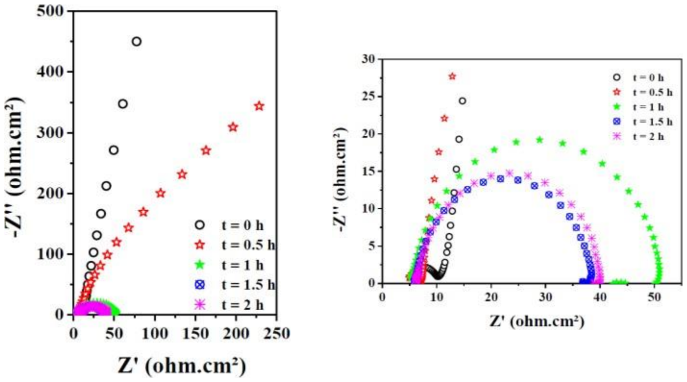

Figure 4. Impedance diagrams in H_2SO_4 pH0.3, at different immersion times of PANI coated. Synthesis time: 6 hours

It can be seen that the immersion time has a significant effect on the impedance of PANI coatings. Result of impedance plots obtained at a short immersion time shows a linear region which means that film behaves as a blocked electrode [8] exhibiting the characteristics of a corrosion reaction inhibited by mass transfer limitations [16]. PANI act as a barrier against the diffusion of the electrolyte (H_2SO_4) and aggressive ions (SO_4^{-2}), protecting the metal.

When the immersion time is longer, the linear region is transformed into a semicircle possibly having the characteristics of a diffusion impedance and attributed to various factors related to the corrosion behavior of the metal in the given environment. The size of the loop corresponds to the charge transfer resistance R_{ct}, and the increase in the values of the capacitance C_{dl} shown on the figure 5 may be due to acid attack on metal [17, 18].

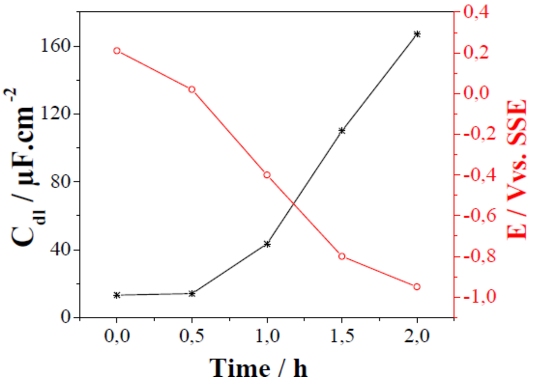

Figure 5. Evolution of the capacity and the free potential as a function of immersion time.

C. Influence of MoO_4^{-2} concentration

Results of corrosion tests carried out on PANI-MoO_4^{-2} films doped with molybdate ions at different concentrations are shown in figure 6. We see that the coatings doped with molybdate ions provide a clear improvement which is traducted by a significant increase of the protection time. This behavior has already been observed in the works by Ohtsuka and al. [19] on films from polypyrrole. The presence of molybdate ions in coating seems to stabilize the passive film on surface of steel.

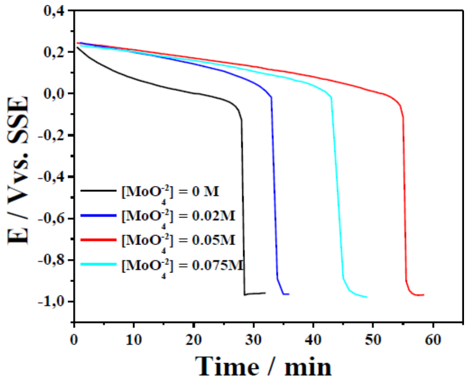

Figure 6. OCP curve versus time in H_2SO_4 pH 0.5 solution for PANI-coated steel doped with molybdate ions. Synthesis time = 6 h.

We have grouped in Table 2 the quantity of electricity applied and the protection time values to the different concentrations of molybdate studied. A better protection of the steel was obtained for an optimal concentration of 0.05 M.

Table 2. Quantity of electricity consumed Qp for current density i = 2 mA.cm-2 at different concentartions of MoO_4^{-2}.

Na_2MoO_4 concentration (M)	0	0.02	0.05	0.075
Q_p (mC.cm^{-2})	556	5231	1712	2894
Protection time (min)	28	34	55	45

IV. Conclusions

This study allowed us to identify the most appropriate experimental conditions for the synthesis of organic coatings based on polyaniline on a steel surface. The coatings are able to offer protection in the acidic medium H_2SO_4.

An improvement in the performance of these coatings has been proposed by doping anions in the structure of the films produced. This improvement could be the result of self-healing of the underlying passive layer. As a result, when the steel surface is attacked by corrosive agents, the conductive polymer is reduced resulting in the expulsion of counter anions. These once released can self-repair the film by the in-situ formation of a passive layer at the site of the lesions.

These findings suggest that doping polyaniline coatings holds promise for corrosion protection of steel, although further research is needed to fully understand the mechanisms and optimize the effectiveness of these coatings.

The use of conducting polymers in corrosion protection offers a promising avenue for addressing the challenges associated with metal corrosion, providing innovative solutions for preserving the integrity of metal surfaces.

Conflict of interest

The authors declare that they have no known competing financial interests or personal relationships that could have appeared to influence the work reported.

References

[1] E. M. Fayyad, S. H. Sanad, A. A. Ismail. Coatings of Conducting Polymers for Corrosion Protection of Mild Steel. Silicon 9, 901-915, (2017).

[2] F. Assassi, N. Ouis, N. Benharrats, M. Kameche. An Investigation on the Corrosion Protection of Mild Steel by Using the Conducting Polymer Polyaniline: Chemical and Electrochemical Studies. Polymer Science Series A 65, 137–146, (2023).

[3] E. M. Fayyad, S. H. Sanad, A. A. Ismail. Coatings of Conducting Polymers for Corrosion Protection of Mild Steel. Silicon 9, 901–915, (2017).

[4] T. Zhang, C. Zeng. Corrosion protection of 1Cr18Ni9Ti stainless steel by polypyrrole coatings in HCl aqueous solution. Electrochimica Acta 50, 4721-4727, (2005).

[5] B. Wessling. From conductive polymers to organic metals, Chemical innovation 31, 34-40, (2001).

[6] I. L. Lehr, S. B. Saidman. Corrosion protection of iron by polypyrrole coatings electrosynthesised from a surfactant solution. Corrosion Science 49, 2210-2225, (2007).

[7] D. W DeBerry. Modification of the Electrochemical and Corrosion Behavior of Stainless Steels with an Electroactive Coating. Journal of the Electrochemical Society 132, 1022,(1985).

[8] M. C. Bernard, S. Joiret, A. Hugot-Le Goff, P. V. Phong. Protection of iron against corrosion using a polyaniline layer. I. Polyaniline electrodeposit. Journal of the Electrochemical Society 148, B12 – B16, (2001).

[9] Y. Zhang, Y. Shao, X. Liu, C. Shi, Y. Wang, G. Meng, X. Zeng, Y. Yang. A study on corrosion protection of different polyaniline coatings for mild steel. Progress in Organic Coatings 111, 240-247, (2017).

[10] Y. Gao, J. Ali Syed, X. Meng, Anti-corrosive performance of electropolymerized phosphomolybdic acid doped PANI coating on 304SS. Applied Surface Science 360, 389-397, (2016).

[11] V. Karpakam, K. Kamaraj, S. Sathiyanarayanan, G. Venkatachari, S. Ramu. Electrosynthesis of polyaniline–molybdate coating on steel and its corrosion protection performance. Electrochimica Acta 56, 2165-2173, (2011)

[12] R. Aitout, L. Makhloufi, B. Saidani. Kinetics of copper electrodeposition onto Polypyrrole films previously synthesised onto iron in oxalic aqueous solution. Application to electrocatalysis Thin Solid Films 515, 1992-1997, (2006)

[13] D. Oukil, L. Benhaddad, R. Aitout, L. Makhloufi, F. Pillier, B. Saidani. Electrochemical synthesis of polypyrrole films doped by ferrocyanide ions onto iron substrate: Application in the electroanalytical determination of uric acid. Sensors and Actuators B 204, 203–210, (2014).

[14] J. Adamski, J. Kochana. Polypyrrole Layers Electrodeposited from TRIS Buffer Solution as Matrix of Tyrosinase Biosensor. Acta Chimica Slovenica 55, 623–626, (2008).

[15] M. Gvozdenovic, B. Jugovic, D. Jambrec, J. Stevanovic, B. Grgur. Application of polyaniline in corrosion protection of metals. ZAŠTITA MATERIJALA 53, broj 4, (2012)

[16] P. Li, T.C. Tan, J.Y. Lee. Corrosion protection of mild steel by electroactive polyaniline coatings. Synthetic Metals 88, 237-242, (1997).

[17] A.S. Patel, V.A. Panchal, G.V. Mudaliar, N.K. Shah. Impedance spectroscopic study of corrosion inhibition of Al-Pure by organic Schiff base in hydrochloric acid. Journal of Saudi Chemical Society 17, 53-59, (2013).

[18] A. Ansari, M. Manssouri, A.Laghchimi, M. Znini, Z. Lakbaibi, M. Azrour. Experimental and theoretical study on corrosion inhibition of new synthesized menthone derivatives (Menthopyrazole compounds) for mild steel in 1 M HCl solution. Mediterranean Journal of Chemistry 10, 62-76,(2020).

[19] T. Ohtsuka, M. Iida, M. Ueda. Polypyrrole coating doped by molybdo-phosphate anions for corrosion prevention of carbon steels. Journal of Solid State Electrochemistry 10, 714,(2006).

Biopolymer Applications Journal **Soumia BOUCHAKHCHOUKHA et al, Vol 03. N°1, 2024, pp. 21-24**
e-ISSN : 2800-1729

STUDY OF L/D RATIO EFFECT ON RESIDUAL HOOP STRESS EVOLUTION IN POLYETHYLENE PIPE

Soumia BOUCHAKHCHOUKHA[1,3*]; Latifa ALIMI[2,3]; Kamel CHAOUI[3]

[1]*National Higher School of Technology and Engineering (ENSTI), 23005, Annaba, ALGERIA;*
[2]*Research Centre in Industrial Technologies CRTI P.O. Box 64, CHERAGA, ALGERIA;*
[3]*LR3MI, Mechanical Eng. Dept, BADJI MOKHTAR University of Annaba (UBMA), P.O. Box 12, Annaba 23000, ALGERIA;*
**Corresponding author email: s.bouchakhchoukha@ensti-annaba.dz*

Received: 26 November, 2023; Accepted: 24 December, 2023; Published : 28 January, 2024

Abstract

In extrusion process of polyethylene tubes, it is known that residual stresses are the consequences of manufacturing process, which requires homogeneous geometric dimensions of diameter and thickness. These impose rapid cooling from the outer tube surface. Ring specimens' were cut along a generatrix from a High Density Polyethylene (HDPE) tube to evaluate the residual stress evolution. Technique used in experiments as presented in a later study, involves on assessing residual deformation as function of ratio (L/D) over a period of time. Then, after determining the creep modulus, residual stress was measured for each ratio (L/D). Deformation values increase towards a plateau after 120h, showing a trend approaching a constant over time. This result is corroborated further by L/D=2, the greater is the diameter, the more this pattern is supported. We can presume that the deformations progress towards a condition of plane deformation. Strain-time curves show typical creep behavior of semi-crystalline viscoelastic materials such as HDPE. Results indicate that the calculated residual hoop stress is negative. In plastic pipe manufacturing, low quench water temperature results in high compressive residual stress at the outer pipe surface.

Keywords: *HDPE, Extrusion, Ratio (L/D), Creep modulus, Residual hoop stress.*

I. Introduction

High Density Polyethylene (HDPE) ranks third in the world by volume among commodity plastics, after polyvinyl chloride and polypropylene. The HDPE market is expanding, with production and demand expected to increase sharply between 2022 and 2027. Asia continues to be the preferred place for demand. The recent expansion of the polyethylene sector has pushed manufacturing centers to relocate to regions with access to raw materials, such as the Middle East, or to regions with strong domestic demand, such as mainland China [1]. Numerous sectors have seen a surge in the utilization of polymer materials. Applications utilizing pressure pipes, such the distribution of natural gas, the purification of drinking water, and the disposal of wastewater, are recognized as examples of large-scale technological advancement. In fact, because of their appealing mechanical qualities, affordable production costs, and simplicity of processing, customers have chosen this class of materials. Polymer constructions need to be sized and manufactured correctly in order to endure the numerous mechanical and/or environmental loads to which they are subjected during their service [2]. We may mention two industrial thermoplastic shaping processes: injection and extrusion molding, the latter of which is primarily utilized in the manufacturing of long items like polyethylene connectors. The idea is to use an extruder to melt and plasticize polymer grains, then an extrusion head to shape the material [3]. It is acknowledged that residual stresses and morphological variations in extruded tubes result from the manufacturing process, which necessitates homogeneous geometric dimensions in terms of thickness and diameter, which calls for quick cooling. As a result, during the extrusion process, the tube's outer layers experience compressive stresses while its inner layers experience positive stresses. These residual stresses play a major role in determining the resistance to crack propagation. Additionally, it has been demonstrated that in outer layers that are subject to compressive residual stresses, the propagation of cracks is slower [4,5]. It is well known that residual stresses from manufacturing processes are present in all polymer tubes. Depending on the manufacturing processes used, residual stresses can vary greatly in size and distribution. In the course of cooling, differential shrinkage across the tube wall is one of the primary causes of residual stress [6]. The residual stresses in polyethylene pipes are calculated in this study using an experimental methodology. In fact, L/D ratio where L and D are ferrules length and diameter and the change in creep modulus are used to measure these stresses.

II. Material and methods

Material

In this study, high-density polyethylene (HDPE-100) material was employed, it was manufactured by the Algerian plastic pipe company TUBOGAZ of ANNABA in its tubular form, they have a standard dimension ratio of 17 and two diameters of 90 mm and 110 mm, and they are designed for the distribution of drinking water [7].

Table 1. Technical Specifications of HDPE-100 [7]

Properties	Values	Standards
Density [kg/m³]	956- 961	ISO 1183
Melt Flow Index MFI [g/10min]	0.2- 0.5	ISO 1133
Young's Modulus[N/mm²]	~ 1200	DIN 53457
Failure Stress [N/mm²]	~ 24	ISO 6259
Failure Strain [%]	>500	ISO 6259
Hardness Shore at 20°C [-]	59	ISO 868
Resilience at 23°C [J/m²]	>600	ASTM D256
Ultimate Elongation (%)	≥350	-
Yield Elongation at 23°C (%)	9	-

Ring slitting method

The method for preparing test specimens involves slitting or cutting the tube on a universal turning machine altering the longitudinal progress. A wooden mandrel is created to retain the tube during machining. High speed steel with a thickness of 5 mm is the cutting material. A speed of 45 rpm is chosen to reduce the impact of the generated heat during cutting at 25°C (Fig 1).

The chosen specimens are shaped like rings of various widths, as seen in Fig 1 (c). Using a cutter blade attached in the tool holder and a slow rotating speed, the two pipes are formed into rings. The widths of the specimens, which were machined from two 110 and 90 mm tubes, are a function of the diameter. L/D = (0.1, 1, and 2) is one of the eight L/D ratios examine [8].

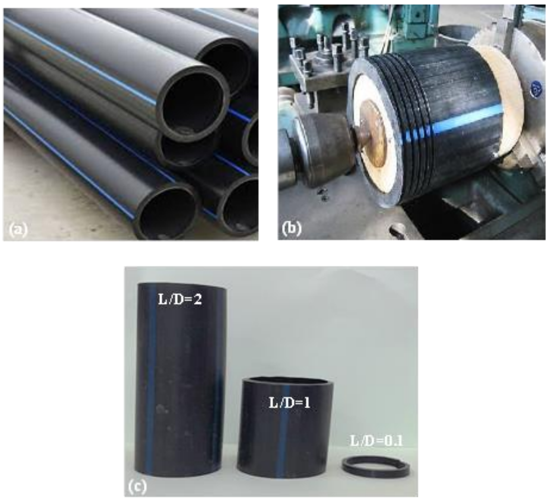

Figure1. Ring slitting method, (a): HDPE Pipe, (b): Pipe cutting operation, (c): Specimens in rings shape.

Residual displacement

The behavior-deformation as a function of diameter D and ratio L/D in time is the center of the observations made during the experiment.

Three ratio cuts from the 90 mm and 110 mm diameter tubes are used to represent the deformations as a function of time. As expected, it is seen that the deformation rises with t and approaches a nearly constant plateau at t around 7 days.

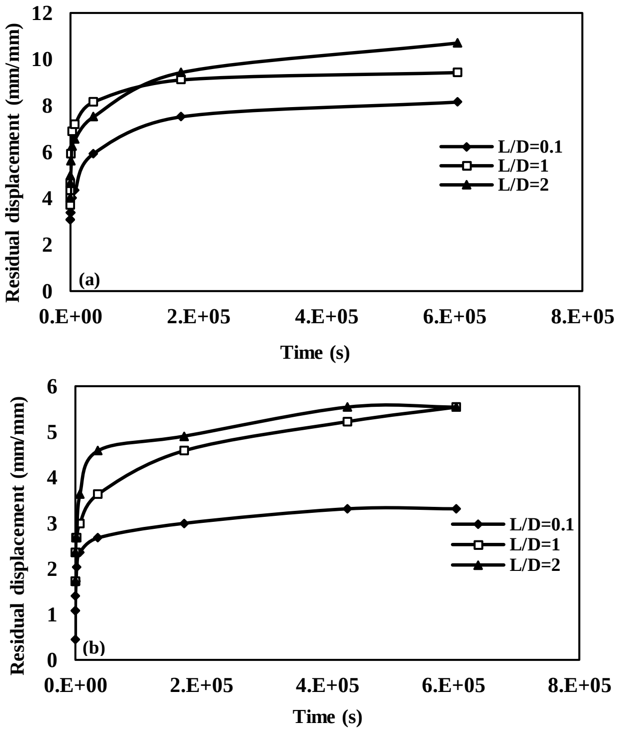

Figure2. Residual displacement vs. time curves for diameters: (a) D 90mm, (b) D110 mm.

III. Calculation approach

Residual stress measurements

The residual stress is based on the deflection that shows the change in the periphery of the ring which decreases or increases over time. By measuring the ring diameter at a specific time, the maximum residual hoop stress can be calculated by the relation (1) developed by Broutman et al., [9].

$$\sigma(Max) = \pm \frac{E(t)h_0}{1-\nu^2}\left(\frac{D_1(t) - D_0}{D_1(t).D_\circ}\right) \qquad (1)$$

Where:

$\sigma_{(Max)}$: Maximum residual hoop stress, (MPa)
E (t): Creep Modulus at time t, (MPa),
h_0: Pipe thickness, (mm),
D_0: Mean diameter before slitting, (mm),
D_1 (t): Mean diameter after slitting at time t, (mm),
t: Time, (hours),
ν: Poisson ratio.

Creep modulus

The Creep modulus can be calculated using the relation (2) developed by Broutman et al., [9], with the constants a = -49.32 and b =509.99 taken from curve shown in (Fig3).

$$E(t) = a\ln(t) + b \quad (2)$$

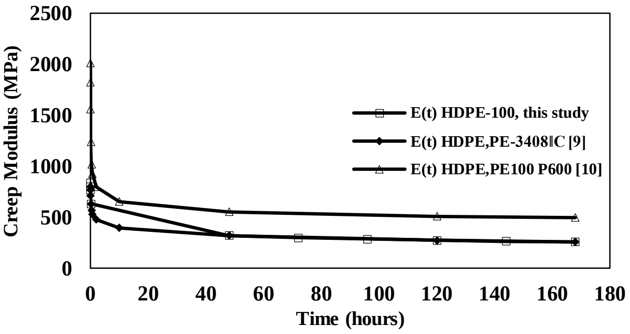

Figure3. Creep modulus E (t) vs. time for HDPE in comparison with literature.

Plastics display distinct viscoelastic behavior, i.e. the reaction to a mechanical load depends not lone on temperature but similarly on time. The time-delayed deformation owing to a constant external load is devoted to as creep. The creep modulus curve was an upper limit curve agreeing to 0 applied stresses resulting from the creep modulus curves found in the literature because creep modulus increases with decreasing applied stress and there is no applied stress during the residual stress measurements [10]. Figure 3 shows a summary of available creep modulus values of thermoplastic materials, especially HDPE [9,10].

Creep is the physical phenomenon which causes the delayed irreversible deformation, i.e. not instantaneous, of a material subjected to a constant stress (thermal or mechanical), even lower than the elastic limit of the material. For a period of time, creep modulus is high enough in the short term, and it is reduced in the long term. The creep behavior can be separated in primary creep with regressive behavior where the creep rate decreases and a secondary creep where the creep rate is almost constant (Fig.3).

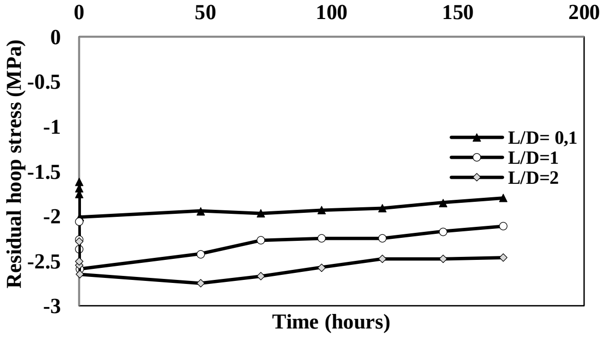

Figure4. Residual hoop stress vs time, D 90mm.

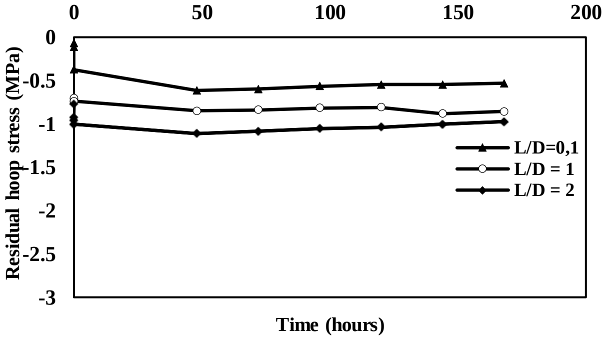

Figure5. Residual hoop stress vs time, D 110 mm.

Fig. 4 and Fig. 5 describes variations of the maximum residual hoop stress on the outer surface vs. time after the ring-slitting, which are resultant of substituting the variations of creep modulus in Fig. 3 into the Eq. (1). From the calculated values, it can be found that residual hoop stresses close to outer surface are compressive. These compressive residual stresses are common phenomenon of the HDPE pipes manufactured by extrusion process [4]. As depicted in Fig.4 and Fig. 5, after the ring-slitting, total values of the maximum residual hoop stresses instantly increase and then slowly increase. After more than 120hours (5 days) the maximum residual hoop stresses are almost constant.

For the tube with a diameter equal to 90 mm, and in the three ratios studied, we found that the value of the residual stress varies from -1.61MPa to -1.79MPa when L/D=0.1, from -2.05MPa to -2.11MPa when L/D=1, and finally from -2.28MPa to -2.46MPa at L/D=2 (Fig. 4).

In the second case studied, where the diameter is equal to 110mm, and in the three ratios we found that the value of the residual stress varies for example in the case where L/D=0.1 from -0.06MPa to 0.53MPa, when L/D=1 it varies from -0.71MPa to -0.85MPa, and for L/D=2, it varies from -0.77MPa to -0.97MPa (Fig. 4).

IV. Conclusions

In this work, experimental approach was used to evaluate residual stresses in polyethylene pipes at two distinct diameters (i.e., 90mm and 110mm), and for three different ratios (L/D) = (0.1, 1, 2). The experimental procedure consists of measuring the deformation over time in relation to the width (length) and diameter of the test piece:

1. Extruded HDPE pipes exhibit compressive negative residual stress.

2. For tube with D=90 mm, in the three ratios studied, values of residual stress varies from -(1.61 to 1.79)MPa for L/D=0.1, from -(2.05 to 2.11)MPa for L/D=1, and from -(2.28 to 2.46)MPa at L/D=2.

3. For D= 110mm, residual stress varies for L/D=0.1 from -(0.06MPa to 0.53)MPa, when L/D=1 it varies from -(0.71 to 0.85)MPa, and for L/D=2, it varies from -(0.77MPa to 0.97)MPa.

4. After ring-slitting, global values of residual hoop stress instantly increase and then slowly increase. Later more than 120 hours residual hoop stress values are almost constant.

References

[1] https://www.ihs.com/products/high-density-polyethylene-chemical-economics-handbook.html
[2] L. Alimi. Comportement mécanique de nouvelles résines HDPE dans des milieux agressifs, Thèse, 2016.
[3] C. Devilliers. Dégradation chimique du PE et influence sur le comportement, l'endommagement et la rupture en fluage : Application à la durabilité d'une canalisation sous pression, Thèse, 296 p., 2011.
[4] K. Chaoui, A. Moet, A. Chudnovsky. Effect of Residual Stress on Crack Propagation in MDPE pipes. Journal of Materials science 22, 3873-3879, 1987
[5] T.R.U. Kratochvilla, H. Muschik, H. Dragaun, Experiences with modified test conditions for notch pipe testing, Polymer Testing 27, 158-160, 2008.
[6] J. Zhang. Experimental Study of Stress Cracking in High Density Polyethylene Pipes, Thèse, 179, 2005.
[7] TUBOGAZ of ANNABA, Algerian plastic pipe company.
[8] S. Bouchakhchoukha, N. Daoudi, L. Alimi, S. Niou, A. Merabtine. Étude de la variation des contraintes résiduelles dans un tube en polyethylene, International Conference on Mechanical Sciences, 12-13 Nov. 2021,Oum El Bouaghi, Algeria.
[9] S. Choi, L. Broutman. Residual stresses in plastic pipes and fittings, effect of annealing on deformation and fracture properties, Polymer Korea21, 93-102, 1997
[10] J. Kim, J. Yoo, Y. Oh. A study on residual stress mitigation of the HDPE pipe for various annealing conditions, Journal of Mechanical Science and Technology29 (3), 1065-1073, 2015

Biopolymer Applications Journal **_Samira Sahi et al. Vol 03. N°1, 2024, pp. 25-28_**
e-ISSN : 2800-1729

Physical and mechanical behavior of poly(vinyl chloride) reinforced by corn flour

Samira SAHI[1*]; Kenza SADOUKI[2], Asma SAHARI[2], Hocine DJIDJELLI[1]; Amar BOUKERROU[1]

1 Laboratory of Advanced Polymer Materials. Department of Process Engineering. Faculty of technology. University A. Mira of Bejaia. Bejaia (06000). Algeria.

2 Laboratory Valuation of Fossil Fuels, Department of Chemical Engineering, National Polytechnic School of Algiers, Algeria.
**Corresponding author email; samira.sahi@univ-bejaia.dz*
Received:28 November,2023 ; Accepted:30 December,2023 ; Published : 28 January, 2024

Abstract

In this work it was investigated the incorporation of corn flour (CF) as filler with different content in poly(vinyl cloride) (PVC) in the aim to decrease the plastics wastes in the environment. The corn flour were mixed to the PVC using the technique of calendaring and hot compression. The characterization of those compounds was done using phisyco-mechanical analysis. The results indicated that the increase of the corn flour content in the matrix was responsible for the reduction of the elongation and stress of the resulting composites and increased the stiffness, the hardness and water adsorption if compared with pure PVC.

Keywords: *Polyvinyl chloride, corn flou, composite materials, physico-mechanical properties*

I. Introduction

In recent years, the use of composite materials has seen considerable development in different areas; aeronautics, automobiles, packaging, construction, etc.

A considerable part of these innovative materials is intended for the packaging sector, in order to replace plastic materials which are used over a very short period of time and which quickly generate a significant volume of waste.

Recent advances in composite science and the development of natural reinforcements offer significant opportunities to develop new materials from renewable resources [1, 2].

Among the plastic materials most used for the preparation of organic composites is polyvinyl chloride (PVC). The latter is one of the most produced plastic materials. Its global production is 35 million tonnes per year. It is a thermoplastic polymer widely used in various sectors, it is ranked third in terms of tonnage after polyethylene (PE) and polypropylene (PP) [3]. In this context, we have chosen to reinforce this thermoplastic polymer (PVC) with corn flour, which is a vegetable filler.

The choice of using this filler was based on the fact that it naturel reinforcement and it has low cost compared to corn starch. So, the corn flour can be valorized by introducing them into a thermoplastic matrix such as PVC. The resulting materials can be used in a several domains, such as packaging.

However, further studies on the reinforcement of PVC with other filler such as ligno-cellolic fibers are being carried out by several researchers [4-5].

The aim of the present study is to study the phisyco-mechanical properties of polyvinyl chloride (PVC) matrix composites reinforced with corn flour (CF), using a variety of analytical techniques such as: tensile test, hardness test, density test and water absorption measurement.

II. Material and methods

II.1 Materials

The different PVC/corn flour formulations developed for this study were based on PVC from type SE-120 supplied by the company CABEL “Cableworks electric” from Algiers, Algeria. This polymer has the properties physical values: K-Wert, from 70.2 to 72.0; a density of 0.52. Additives have been added for the preparation of the different formulations and which are the phthalate of dioctyl (DOP) as a plasticizer, a thermal stabilizer based on Ca/Zn and stearic acid as lubricant. Corn flour with a particle size ≤ 100 µm and a relative humidity of 7% was provided by the company AGRO CEREAL/Moulin Royal Akbou, Algeria. PVC type SE-1200 was used as a matrix for the production of composites.

II.2 Methods

Determination of dry matter and moisture content of corn flour

A mass of CF is weighed (P_0) into a ceramic mass crucible (P_1). It is placed in an oven at 105°C. After 24 hours, the crucible is removed from the oven and weighed (P_2). The dry matter content is given by the following formula:

$$\% \, DM = \frac{P_2 - P_1}{P_0} * 100 \quad (1)$$

The moisture content (Mc) is determined by the following expression:

$$\% \, Mc = 100 - \% \, DM \quad (2)$$

The density of corn flour (d_{CF}) is determined by pycnometer method using the relation (3):

$$d_{éch} = \frac{W_2}{W_1 + W_2 - W_3} \, d_{water} \quad (3)$$

With :
w_1 : the mass of the pycnometer full of liquid (water) (gr).
w_2 : mass of CF (gr).
w_3: mass of pycnometer full of liquid with CF immersed (gr).
d_{water}: density of the liquid used (water).

Samples preparation

The different formulations presented in Table 1 were prepared by two transformation processes, namely: calendaring and compression molding. The PVC and its additives were introduced into a T6HK8 type turbo-mixer for 15 min. The resulting mixture is introduced into a two-roll mixer at a temperature of 140°C. Then, the filler (PCF) is added to obtain the mixture for each formulation.

The prepared mixture is introduced into the plates of the TONJINE brand table press at a temperature of 170° C under a pressure force of 300 kN for 5 min. Plates of 250×250×2 mm^3 are obtained and cooled to room temperature, which will be used for cutting samples in the form of dumbbells.

Table 1. Mass composition of the different formulations.

Formulations Products	F0	F10	F20	F30
PVC compound	100	90	80	70
CF	0	10	20	30

Water absorption test

The water absorption test is carried out according to ASTM D7031-04. The samples immersed in distilled water at room temperature with stirring. The samples are weighed every 24 hours until their mass is stabilized. The variation of mass is given by the following formula :

$$WA(\%) = \frac{w - w_0}{w_0} \times 100 \qquad (4)$$

where :
WA : the water absorption (%),
W : the final mass of the sample
W_0 : the initial weight of the sample

Density test

Sample density was determined using a DSM density Meter.

Tensile testing

The mechanical behavior of the composites produced was determined using an MTS Criterion tensile testing machine, in accordance with NFC 32-200.

For each formulation five specimens were tested. As a result, Young's modulus, strain and stress were determined.

Shore D hardness test

Shore D hardness is measured by applying a force the pointed steel needle of a shore D durometer, on plates of shore D durometer, on 5x5 cm^2 plates of a different thickness.

III. Results and discussion

Physical properties of corn flour

The results recorded (Table 2) show that the density of CF is 1.58. This result is similar to the density values given by Benjamin et al. [6], which is 1.62.

Dry matter content and moisture content are 88.37% and 11.63% respectively. These results corroborate previous research [6, 7].

Table 2. Physicochemical characteristics of corn flour.

Caracteristics	CF
Density	1,58
Mc (%)	11,63
DM (%)	88,37

Water absorption test

The evolution of the water absorption of PVC and PVC/CF composites as a function of filler ratio and immersion time in distilled water is illustrated in figure 2. The results show that the water absorption of virgin PVC is negligible, due to the hydrophobic nature of this polymer, whereas the addition of filler to the PVC matrix increases water absorption with increasing filler ratio and immersion time in distilled water. This can be explained by the presence of hydroxyl groups in starch (a major constituent of corn flour). These groups form hydrogen bonds with water molecules, giving starch-based materials their hydrophilic character. The higher the loading rate, the higher the OH concentration in the composites, and the greater the rate of water absorption. The water absorption rate after 34 days' immersion is 0.27% for virgin PVC and 2.19, 4.8 and 10.7% for F10, F20 and F30 formulations respectively. Similar results have been recorded by several authors who have introduced plant fillers into different hydrophobic matrices [8, 9].

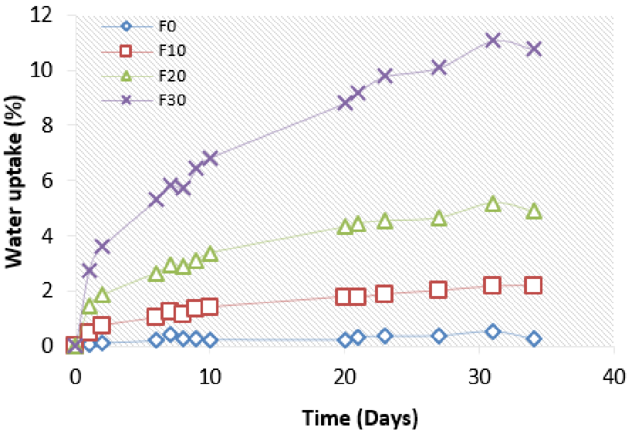

Figure 1. Evolution of the water uptake of PVC and PVC/CF composites.

Density test

The results of the density test on PVC/FM composites as a function of filler ratio are shown in Fig. 4. It is clear that the addition of corn flour to the PVC matrix results in a slight increase in density, which is not significant. It increases from 1.23 for PVC compound to 1.25, 1.25 and 1.27 for filler contents of 10, 20 and 30% respectively. This is explained by the fact that CF has a low density (Table 2). This result is in agreement with the results recorded by Kormin et al. [8] who introduced different types of starch as filler in LDPE.

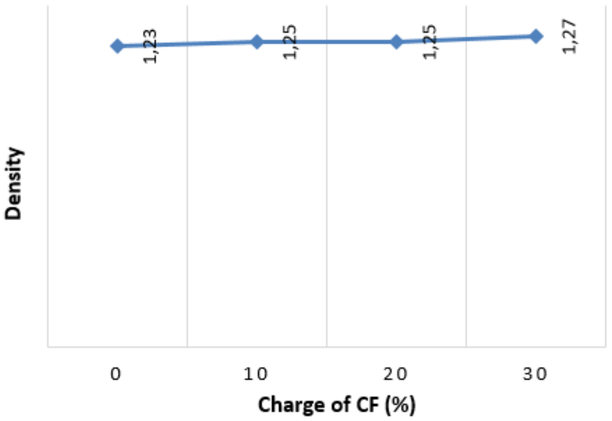

Figure 2. Density of PVC and composites PVC/CF with 10, 20 and 30% of the charge.

Tensile testing

The comparison in tensile properties of pure PVC and PVC reinforced with CF for different formulations is illustrated in figure 3.

For tensile strength (Figure 3-a), a decrease in this property is recorded with the introduction of CF into the PVC matrix. A decrease of 36.38%, 48% and 67.48% is recorded for F10, F20 and F30 formulations respectively, compared with unfilled PVC. These results are in agreement with those obtained by other researchers who have worked on LDPE/corn starch composites [7]. They explained this result by the tendency of corn flour particles to group together, forming agglomerates that induce heterogeneities and non-uniform stress transfer within the matrix, resulting in material embrittlement.

Figure 3-b shows the Young's modulus of PVC/CF composites as a function of filler ratio. These results indicate that the introduction of filler into the matrix increases the stiffness of the materials in formulations F10 and F20, which translates into an increase in Young's modulus, but a decrease is recorded in formulation F30. This can be explained by the rigid nature of CF compared with soft PVC. Above 20% plant filler, there is poor dispersion of this filler in the polymer matrix. At high filler contents, the material becomes rough and the surface cracks [10].

For elongation at break, it can be seen that this parameter tends to decrease significantly with the introduction and increase of filler content into the matrix. The elongation at break drops from 118.75% for PVC to 75.99%, 61.99% and 33% for composites filled with 10, 20 and 30% CF respectively. Similar results were observed for LDPE/starch [7] and PVC/wood pulp composites [11].

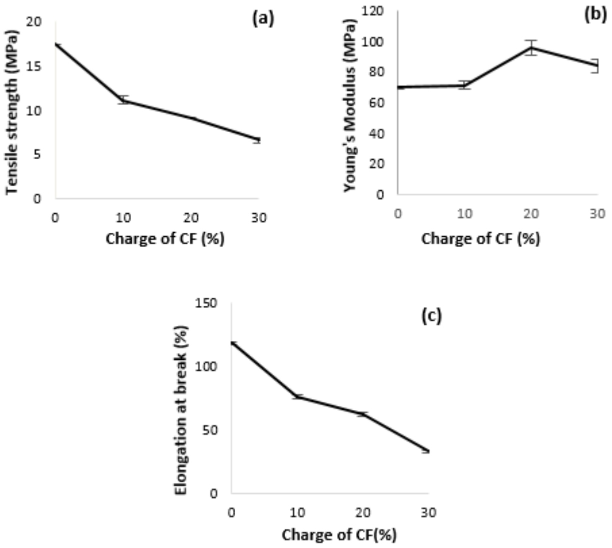

Figure 3. Tensile properties of PVC and PVC/CF composites: (a) tensile strength (b) Young's modulus and (c) elongation at break.

Shore D hardness test

Figure 4 shows that the hardness of PVC/CF composites increases as the filler content in the PVC increases. This behavior can be explained by the fact that corn flour is stiffer than soft PVC, consequently, the material gains more resistance to penetration, so the hardness will be higher. This observation is in perfect agreement with others studies [3, 12, 13] which reported similar results.

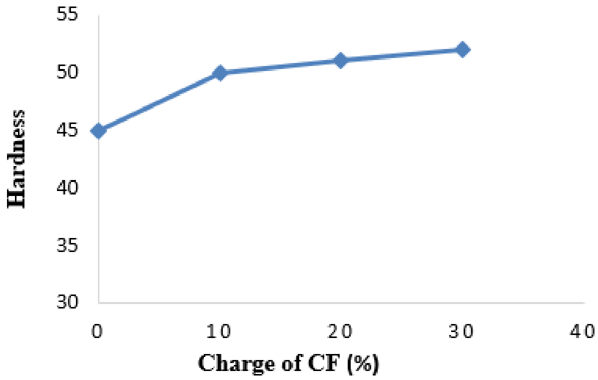

Figure 4. Hardness of PVC and composites PVC/CF with 10, 20 and 30% of the charge.

Conclusions

The results obtained in this study showed that:

- CF has a low density, very rich in dry matter with a low moisture content.
- The introduction of CF as a filler in PVC had no effect on the density of the composites elaborated.
- Water absorption increases with increasing filler content in PVC and immersion time in water.
- A study of the tensile properties of PVC/CF composites showed a decrease in tensile strength and in elongation at break with increasing filler ratio in the PVC matrix. On the other hand, an increase in stiffness was recorded.
- The hardness of composites elaborated increased with increasing CF filler ratio in the PVC.

Although the properties of some blends are acceptable for certain applications, further improvements will be needed, mainly by optimizing the characteristics of the charge-matrix interface.

Conflict of interest

The authors declare that they have no conflict forfinancial interests or personal relationships that howcan influence the work reported in this paper.

References:

[1] L. J. Zhang, Li. P. Peng, F. Bian. Microwave-assisted solvent-free acetylation of cellulose with acetic anhydride in the presence of iodine as a catalyst. Molecules 14, 3551-3566, 2009

[2] S. Thomas, S.A. Paul, L.A. Pothan, B. Deepa, Cellulose Fibers: Bio- and NanoPolymer Composites, Green Chemistry and Technology 3-42, 2011

[3] S. Sahi, H. Djidjelli, S. Touazi, Amar Boukerrou. Valorisation des déchets ligno-cellulosiques pour la préparation d'un nouveau matériau composite PVC/farine des noyaux de dattes. Matériaux et techniques 109, 102, 1-10, 2021

[4] B.L. Shah, L.M. Matuana, P.A. Heiden, Novel coupling agents for PVC/wood-flour composites, Journal of Vinyl and Additive Technology 11, 160-165, 2005

[5] Y.T. Zheng, D.R. Cao, D.S. Wang, Study in the interface modification of bagasse fibre and the mechanical properties of composite with PVC, Composites: Part A 38, 20-25, 2007

[6] B. L. Johnson, M. R. Holland, J.G. Miller, J. I. Katz. Ultrasonic Attenuation and Speed of Sound of Cornstarch Suspensions. The Journal of the Acoustical Society of America 133, 1399-1403, 2013

[7] S. Sahi, H. Djidjelli, A. Boukerrou. Biodegradation study of bio-corn flour filled low density polyethylene composites assessed by natural soil. Journal of Polymer Engineering 36, 245-252, 2015

[8] S. Kormin, F. Kormin, M. D. H. Beg, B. M. P. Mohd. Physical and mechanical properties of LDPE incorporated with different starch sources. Materials Science and Engineering 226, 012157, 2017

[9] Sahi, S. Djidjelli, H. Utilisation de l'amidon comme charge biodégradable dans les matériaux composites polyéthylene basse densite/amidon. Annale de Chimie et Science des Matériaux 38, 189-202, 2013

[10] H. Djidjelli, A. Boukerrou, A. Rabouhi, R. Founas, M. Kaci, O. Zefouni, N. Djillali, L. Belmouhoub. Effect of olive residue benzylation on the thermal and mechanical properties of poly (vinyl chloride)/olive residue composites. Journal of Applied Polymer Science 7, 1459-1455, 2008

[11] N. Sombatsompop, K. Chaochanchaikul, C. Phromchirasuk, S. Thongsang. Effect of wood sawdust content on rheological and structural changes, and thermo-mechanical properties of PVC/sawdust composites. Polymer International 52, 1847-1855, 2003

[12] S. Nedjema, H. Djidjelli, A. Boukerrou, N. Chibani, Effet du désencrage et d'un traitement de surface sur les propriétés mécaniques des composites PVC/fibre de papier journal, Annale de Chimie et Sciences des Matériaux 37, 201-214, 2012

[13] M. Khali, Z. Boussena, L. Boutekrabt, Effet de l'incorporation des noyaux de dattes sur les caractéristiques technologiques et fonctionnelles de la farine de blé tendre, Nature et Technologie 12, 15–25, 2015